CHEMISTRY AND TECHNOLOGY OF MEDICINAL COMPOUNDS AND BIOLOGICALLY ACTIVE SUBSTANCES

ХИМИЯ И ТЕХНОЛОГИЯ ЛЕКАРСТВЕННЫХ ПРЕПАРАТОВ И БИОЛОГИЧЕСКИ АКТИВНЫХ СОЕДИНЕНИЙ

ISSN 2686-7575 (Online)

https://doi.org/10.32362/2410-6593-2022-17-2-107-130

UDC 547.1

REVIEW ARTICLE

Bifunctional gallium cation chelators

Anna G. Polivanova✉, Inna N. Solovieva, Dmitrii O. Botev, Danil Y. Yuriev, Alyona N. Mylnikova, Maxim S. Oshchepkov

D.I. Mendeleev Russian University of Chemical Technology, Moscow, 125047 Russia
✉Corresponding author, e-mail: zagchem@mail.ru

Abstract

Objectives. *The chemistry of ^{67}Ga and ^{68}Ga radionuclides plays a key role in nuclear medicine for applications in radiopharmaceuticals, in particular, in noninvasive in vivo molecular imaging techniques. The use of radiometals for labeling biomolecules typically requires the use of bifunctional chelators, which contain a functional group for covalent bonding with the targeting vector in addition to the polydentate fragment coordinating the metal. The aim of the present review article is to analyze the currently accumulated experimental material on the development and application of bifunctional chelators of gallium cations in medical research, as well as to identify the main requirements for the structure of the chelator and its complexes with ^{68}Ga, which are used to create effective Ga-based pharmaceutical preparations.*

Results. *The review analyzed macrocyclic bifunctional chelators forming stable in vivo complexes with ^{68}Ga and acyclic chelators, whose main advantage is faster complexation kinetics due to the short half-life of ^{68}Ga. The advantages and disadvantages of both types of ligands were evaluated. In addition, a critical analysis of the binding constants and the conditions for the formation of complexes was presented. Examples of the influence of the geometry, lipophilicity, and total charge of the metal complex on the biodistribution of target radiopharmaceuticals were also given.*

Conclusions. *Despite the progress made in the considered areas of bifunctional chelators, the problem of correlating the chemical structure of a metal-based radiopharmaceutical with its behavior in vivo remains important. Comparative studies of drugs having an identical targeting vector but containing different bifunctional chelating agents could help further elucidate the effect*

of metal chelate moiety on pharmacokinetics. In order to create effective bifunctional chelating agents, it is necessary to take into account such factors as the stability and inertness of the chelator and its complexes under physiological conditions, lipophilicity, complexation kinetics, chelation selectivity, combinatoriality of the basic structure, along with economic aspects, e.g., the availability of raw materials and the complexity of the synthesis scheme.

Keywords: *bifunctional chelator, ligand, gallium, radiopharmaceutical*

For citation: Polivanova A.G., Solovieva I.N., Botev D.O., Yuriev D.Y., Mylnikova A.N., Oshchepkov M.S. Bifunctional gallium cation chelators. *Tonk. Khim. Tekhnol. = Fine Chem. Technol.* 2022;17(2):107–130 (Russ., Eng.). https://doi.org/10.32362/2410-6593-2022-17-2-107-130

ОБЗОРНАЯ СТАТЬЯ

Бифункциональные хелаторы к катиону галлия

А.Г. Поливанова✉, И.Н. Соловьёва, Д.О. Ботев, Д.Ю. Юрьев, А.Н. Мыльникова, М.С. Ощепков

Российский химико-технологический университет им. Д.И. Менделеева, Москва, 125047 Россия

✉*Corresponding author, e-mail: zagchem@mail.ru*

Аннотация

Цели. *Химия радионуклидов ^{67}Ga и ^{68}Ga играет одну из ключевых ролей в ядерной медицине для применения в радиофармпрепаратах, в частности, в неинвазивных методах молекулярной визуализации in vivo. Использование радиометаллов для мечения биомолекул обычно требует использования бифункциональных хелаторов, которые, кроме полидентатного фрагмента, координирующего металл, содержат функциональную группу для ковалентного связывания с вектором-мишенью. Цели данного обзора – проанализировать накопленный к настоящему времени экспериментальный материал, касающийся разработки и применения в медицинских исследованиях бифункциональных хелаторов к катиону галлия, а также выявить и проанализировать основные требования, предъявляемые к структуре хелатора и его комплексов с ^{68}Ga, необходимые для создания эффективных фармакологических препаратов на его основе.*

Результаты. *Рассмотрены макроциклические бифункциональные хелаторы, образующие стабильные in vivo комплексы с ^{68}Ga, а также ациклические хелаторы, преимущество которых заключается в более быстрой кинетике комплексообразования, что является ключевым фактором, учитывающим короткий период полураспада ^{68}Ga. Проведена оценка достоинств и недостатков обоих типов лигандов. Кроме того, осуществлен критический анализ констант связывания и условий образования комплексов. Рассмотрены примеры влияния природы металлического комплекса (геометрия, липофильность, общий заряд) на биораспределение целевых радиофармацевтических препаратов.*

Выводы. *Несмотря на достигнутые успехи в рассмотренных направлениях создания бифунциональных хелаторов, по-прежнему важной остается проблема корреляции химической структуры радиофармпрепаратов на основе металлов с их поведением in vivo. В этом отношении сравнительные исследования препаратов, имеющих идентичный вектор нацеливания, но включающих разные бифункциональные хелатируюшие агенты,*

могут помочь в дальнейшем выявлении влияния металл-хелатного фрагмента на фармакокинетику. В целом можно отметить, что для создания эффективного бифункционального хелатирующего агента нужно принимать во внимание целую совокупность факторов, включающую стабильность и инертность хелатора и его комплексов в физиологических условиях, липофильность, кинетику комплексообразования, селективность хеланирования, комбинаторность базовой структуры, а также экономические аспекты: доступность сырья, сложность схемы синтеза.

Ключевые слова: *бифункциональный хелатор, лиганд, галлий, радиофармпрепарат*

Для цитирования: Поливанова А.Г., Соловьёва И.Н., Ботев Д.О., Юрьев Д.Ю., Мыльникова А.Н., Ощепков М.С. Бифункциональные хелаторы к катиону галлия. *Тонкие химические технологии.* 2022;17(2):107–130. https://doi.org/10.32362/2410-6593-2022-17-2-107-130

INTRODUCTION

Unlike other methods such as X-rays, computed tomography (CT) and ultrasound, which predominantly provide anatomical information, non-invasive molecular imaging allows chemical and biological processes to be measured and visualized in living systems.

Nuclear medicine is a molecular imaging technique based around radioactive isotopes used as tracers. The two main imaging techniques used in nuclear medicine are single photon emission computed tomography (SPECT) and positron emission tomography (PET).

Although PET has certain advantages in comparison to SPECT, such as high resolution and sensitivity, as well as the ability to quantitative evaluation due to a standardized attenuation correction method, the use of PET is limited due to the short half-lives of the four traditional standard isotopes: ^{11}C ($t_{1/2}$ = 20 min), ^{13}N ($t_{1/2}$ = 10 min), ^{15}O ($t_{1/2}$ = 2 min), and ^{18}F ($t_{1/2}$ = 110 min). With the exception of ^{18}F, the solution to this problem requires the maintenance of a cyclotron for isotope production in the immediate vicinity of the imaging apparatus. Despite high equipment maintenance costs, the rise in the use of PET imaging over the past decades has been largely driven by the successful use of [^{18}F] fluorodeoxyglucose, helping PET to become an indispensable tool for diagnosing various types of malignant neoplasms. Consequently, PET has evolved from a research tool to a practical, highly efficient clinical imaging technique, which has had a tremendous impact on clinical medicine and pharmaceutical development. This progress has also spurred the development of other imaging techniques such as PET–CT and PET–magnetic resonance imaging, as well as fluorescence imaging.

However, the use of traditional short-living isotopes hinders the study of long-term processes, limiting this method to the study of fast biological processes. For this reason, non-standard PET radioisotopes have been produced and investigated. The wider half-life ranges of such isotopes offer better compatibility with the biological half-lives of certain target vectors used for the development of new radiopharmaceuticals. In this context, radioactive metals such as zirconium, yttrium, indium, gallium, and copper were considered [1].

Gallium-68 (^{68}Ga), which has a half-life of 1.13 h, decays with emission of positrons and capture of electrons (11%). The increased interest in ^{68}Ga is based on its availability from the ^{68}Ge/^{68}Ga generator system, which permits the cost-effective use of ^{68}Ga-based radiopharmaceuticals in clinical centers lacking a local cyclotron. Although ^{68}Ge/^{68}Ga generators were first introduced more than 50 years ago, the most important factor

in the recent growth in the number of ^{68}Ga-based radiopharmaceuticals has been the progress in generators' design. A new generation of these systems is able to produce ^{68}Ga as [^{68}Ga]$GaCl_3$, which solved critical impurity problems and made such generators commercially available. The decay of the ^{68}Ge isotope to ^{68}Ga with a half-life of 270.8 days allows its use to obtain long-living generator systems having an estimated period of 1–2 years for radiopharmaceutical applications.

The use of radiometals for labeling biomolecules usually requires the use of bifunctional chelators (BFC), which bind the metal at one end and contain a functional group for covalent bonding with the targeting vector at the other end (Table).

The choice of BFC is determined by the nature and oxidation state of the metal radionuclide. The optimal BFC should ideally meet the following requirements:

Table. Stability constants (log β_1) and synthesis conditions of $^{67/68}$Ga bifunctional chelating complexes

Chelating agent*	log β_1	$^{67/68}$Ga binding conditions	RCY** (%)	Reference
DOTA (**1**)	21.3	pH = 4.8, 5 min, 95°C	>90	[2]
NOTA (**3**)	30.7	pH = 3.5, 10 min, 95°C	>95	[3]
NODASA (**3a**)	–***	0.5 M CH_3COONH_4, 25 min, 90°C	–	[4]
NODAGA (**3b**)	–	25 min, 95°C	95	[5]
p-SCN-Bn-NOTA (**3c**)	–	pH = 6.0, 10 min, 25°C	89	[5]
NODAPA-OH (**3d**)	–	pH = 2.8, 3 min, 85°C	85	[5]
NODAPA-NCS (**3e**)	–	pH = 2.8, 3 min, 75°C	85	[5]
NODAPA-$(NCS)_2$ (**3f**)	–	pH = 2.8, 3 min, 75°C	–	[5]
TRAP (**3g**)	26.24	pH = 3.0, 3 min, 40°C	95	[6]
NOPO (**3h**)	25.01	2.7 M HEPES, 5 min, 25°C	99	[7]
H_5NOA2P (**3i**)	34.44	pH = 7.4, 30 min, 95°C	–	[8]
H_3NOKA	–	pH = 6.0, 60 min, 25°C	35	[9]
$DATA^p$ (**4a**)	–	pH = 4.7, 1–10 min, 25°C	93	[10]
$DATA^m$ (**4b**)	21.7	pH = 4.7, 1 min, 25°C	97	[10]
$PhDATA^{pph}$ (**4c**)	–	pH = 4.7, 1–10 min, 25°C	93	[10]

Table. Continued

Chelating agent*	log β_1	$^{67/68}$Ga binding conditions	RCY** (%)	Reference
$DATA^{ph}$ (**4d**)	–	pH = 4.7, 1–10 min, 25°C	84	[10]
NO_2Bn-PCTA (**5**)	19.37	pH = 3–5, 25°C	96	[10]
Diamsar (**6a**)	–	0.1 M CH_3COONa, 35 min, 85°C	98	[11]
DiamsarDGA (**6b**)	–	30 min, 85°C	98	[11]
H_2dedpa (**8**)	28.11	0.1 M CH_3COONa, 10 min, 25°C	97	[12]
HBED (**7**)	38.51	pH = 4.2, 4 min, 95°C	99	[13]
HBED-CC (**7a**)	–	pH = 4.2, 4 min, 25°C pH = 4.8, 10 min, 25°C	99 96	[14, 15]
KP46 (**11**)	36.79	pH < 2.0, 25°C	–	[16]
EHP	27.52	pH = 7.4, 15 min, 25°C	–	[17]
EHMP	29.55	pH = 7.4, 15 min, 25°C	–	[17]
CP256 (**14a**)	–	pH = 6.5, 5 min, 25°C	95	[18]
$NTP(PrHP)_3$ (**14c**)	33.34	pH = 7.4, 25°C	98	[19]
DFO (**15**)	28.6	pH = 4.5, 5 min, 25°C	96	[20]
Df-Bz-NCS (**15a**)	–	pH = 7.2, 5 min, 25°C	>90	[21]

* All abbreviations are described below in the text of the article.
** RCY is a radiochemical yield.
***No data is available.

- Stability/inertness: BFC should form thermodynamically stable and kinetically inert complexes to prevent any ligand exchange or hydrolysis *in vivo*.
- Kinetics of rapid complexation: for biological targeting vectors, BFC radiolabeling should be effective and fast at low temperatures and low pH.
- Selectivity: BFC must selectively bind the metal of interest in order to avoid low specific activity during radioactive labeling, for example, due to the presence of other decay products.
- Universal chemistry of conjugation: the flexibility of conjugation of BFC with functional groups of target vectors allows optimizing pharmacokinetics by regulating the polarity of the entire conjugate.
- Affordability: BFC preparation should be simple, fast, cost-effective, and scalable for preparing several grams of product with the minimum possible number of reaction steps.

However, the success of BFC is not guaranteed even while meeting all of the requirements above. The two most important parameters of BFC that affect the properties of radiopharmaceuticals *in vivo* are the total charge and lipophilicity of the corresponding BFC metal complex. These parameters are determined by the geometry and set of BFC donors, as well as by the coordinated radiometal. For example, some peptide targeting vectors conjugated to identical BFC but labeled with different radiometals differ in binding to the receptor and behavior *in vivo* [22].

In recent years, various structural types of chelating agents with high stability and selectivity towards Ga(III) have been proposed for use in *in vivo* diagnostics.

MACROCYCLIC GALLIUM CHELATING AGENTS

In recent years, the development of BFCs in general, as well as chelators to Ga(III), has mainly focused on polyaza macrocyclic ligands (Fig. 1). Such systems minimize transchelation or metal loss *in vivo*, which is beneficial for their use as radiopharmaceuticals.

In order to saturate all coordination sites on the six-coordinated Ga(III) cation, several multidentate derivatives of TACN (1,4,7-triazacyclononane) and cyclene (1,4,7,10-tertraazacyclododecane) with additional thiol-S, carboxylate-O and phosphonate-O donor groups were developed by introducing side branches on the secondary amines of the corresponding

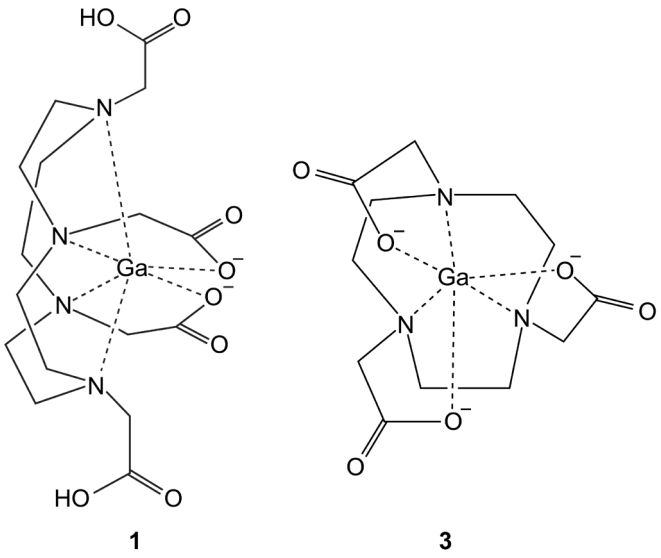

Fig. 1. DOTA (**1**) and NOTA (**3**) complexes with gallium.

macrocycle [23–29]. The most prominent representative of this category is the DOTA (**1**) ligand (1,4,7,10-tetraazacyclododecane-1,4,7,10-tetraacetic acid (Fig. 1). The thermodynamic constant of formation of the Ga-DOTA complex log β_1 = 21.3 is slightly higher than that of the Ga(III)-transferrin complex [2].

A donor set of N_4O_2 of the cyclene fragment and two carboxylate groups encapsulate the metal center in the Ga-DOTA complex with cis-pseudo-octahedral geometry (Fig. 1) [30, 31]. Consequently, Ga-DOTA complexes have a negative overall charge under physiological conditions. Due to the kinetic inertness of the macrocycle, the complexation kinetics of DOTA are slow. Due to DOTA (**1**) radiolabeling requiring conventional or microwave heating to achieve adequate yields and specific activity, its application is limited to thermally stable target vectors [32–34].

Smith *et al.* investigated tunable ^{68}Ga-labelled DO2A-like macrocycles for myocardial perfusion imaging (Fig. 2). By furnishing the DO2A (**2**) pendant arms, it was possible to influence the lipophilicity and charge while retaining a 6-coordination site for Ga^{3+} (Fig. 2). Radiolabelling was carried out at 100°C for 30 min with a pH of 4.93 in a NaOAc buffer [0.2 M, 0.5 mL]. The compounds with the highest lipophilicity [^{68}Ga] GaDO2A-(*xy*-TXP)$_2$ ($logD_{7.4}$ – 0.28 ± 0.01) and [^{68}Ga]GaDO2A-(*xy*)$_2$ ($logD_{7.4}$ – 0.31 ± 0.01) were assessed in an *ex vivo* Langendorff isolated perfused heart model. Uptake in compromised hearts was found to be significantly lower for both ^{68}Ga-labelled complexes than in healthy hearts [35].

The NOTA (**3**) ligand (1,4,7-triazacyclononane-1,4,7-triacetic acid) (Fig. 1), which is rapidly and efficiently radiolabeled at room temperature, is highly stable *in vivo* [36–38]. Due to the smaller size of the corresponding cavity compared to DOTA, triazacyclononane ligands exhibit high conformational and size selectivity with respect to Ga(III). The NOTA (**3**) ligand and its derivatives bind Ga(III) in pseudo-octahedral coordination—N_3O_3 with low deformation, leading to complexes having a neutral total charge at physiological pH (Fig. 1) [39, 40].

The thermodynamic stability of the Ga-NOTA complex (log β_1 = 30.7) is about nine orders higher than that of Ga-DOTA [3]. This results from its excellent incorporation of a small Ga(III) cation into the NOTA (**3**) nine-membered triazamacrocycle cavity. Regarding conjugation to targeting vectors, the use of one side functional group of the carboxylic acid DOTA (**1**) does not affect its ability to bind the metal, since only two of the four available carboxylic acid groups are involved in metal coordination. In the case of NOTA (**3**), conjugation

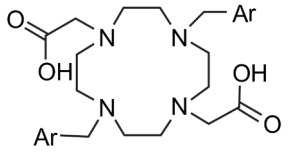

2

DO2A-Bn_2 (**2a**) Ar = Ph

DO2A-xy_2 (**2b**) Ar = m,m'-Xylyl

DO2A-$(xy\text{-}TPP)_2$ (**2c**) Ar = 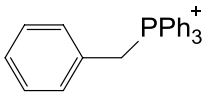

DO2A-$(xy\text{-}TTP)_2$ (**2d**) Ar = 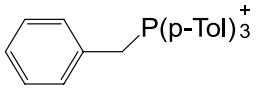

DO2A-$(xy\text{-}TXP)_2$ (**2e**) Ar = 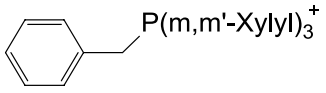

Fig. 2. DO2A (**2**) structural analogues.

can be achieved either using bifunctional derivatives of NOTA or using one of the three available carboxylic acid functional groups. However, if one of the carboxylic acid side groups is used for conjugation, the coordination properties of NOTA (**3**) are potentially impaired due to the impossibility of achieving the preferred stable octahedral coordination.

In order to preserve the hexadentate coordination of NOTA while ensuring covalent conjugation with the target vector, a range of derivatives have been developed: *p*-SCN-Bn-NOTA (**3c**) (S-2-(4-isothiocyanatobenzyl)-1,4,7-triazacyclononane-1,4,7-triacetic acid), NODASA (**3a**) (1,4,7-triazacyclononane-*N*-succinic acid-*N′*,*N″*-diacetic acid), and NODAGA (**3b**) (1,4,7-triazacyclononane-*N*-glutamic acid-*N′*,*N″*-diacetic acid) (Fig. 3). These compounds exhibit high labeling efficiency and stability *in vivo* [4, 39–42].

Other ligands NODAPA-OH (**3d**) and NODAPA-$(NCS)_n$ (**3e**, **3f**) (n = 1–2), which demonstrate radioactive labeling efficiency comparable to NOTA (**3**), are available due to an economical and cost-effective synthesis scheme. At pH 2.8, 85% of all tested ligands were radiolabeled in 3 min at 45°C for NOTA (**3**) and NODAPA-OH (**3d**) and at 75°C for NODAPA-$(NCS)_n$ (**3e**, **3f**). The stability of the corresponding ^{68}Ga complexes was in the same range as the related NOTA, with less than 2% activity loss after 3 h in a rat plasma study. The possibility of using NODAPA-NCS (**3e**) was also demonstrated by conjugation with L-lysine and glucosamine with a yield of 65%–73% [5].

Another approach to the creation of multimeric TACN-based radiopharmaceuticals is *N*,*N′*,*N″*-trisubstituted BFC PrP9(TRAP) (**3g**) (Fig. 4) (1,4,7-triazacyclononan-1,4,7-tris[methyl(2-carboxyethyl) phosphinic acid) using methyl(2-carboxyethyl) phosphinic acid [6].

In accordance with the crystal structure, the PrP9 (**3g**) ligand encapsulates the ^{68}Ga(III) cation with an N_3O_3 donor distorted in an antiprismatic manner due to the amino groups of the macrocycle and side arms of the deprotonated phosphinic acid. Careful analysis of the Ga-PrP9 bond angles, which are close to a perfect octahedron, shows that the Ga-PrP9 complex is less constrained than its structurally related counterparts Ga-NOTA and Ga-NODASA, resulting in the cavity formed by

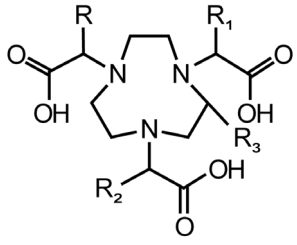

3

NODASA (**3a**) R = CH_2COOH, R_1 = R_2 = R_3 = H

NODAGA (**3b**) R = CH_2CH_2COOH, R_1 = R_2 = R_3 = H

p-SCN-Bn-NOTA (**3c**) R_1 = R_2 = R_3 = H, R_3 = *p*-Ph-NCS

NODAPA-OH (**3d**) R = *p*-Ph-OH, R_1 = R_2 = R_3 = H

NODAPA-NCS (**3e**) R = *p*-Ph-NCS, R_1 = R_2 = R_3 = H

NODAPA-$(NCS)_2$ (**3f**) R = R_1 = *p*-Ph-NCS, R_2 = R_3 = H

Fig. 3. Structural analogues of NOTA (**3**).

PrP9 (**3g**) being a good fit for Ga(III) coordination [32, 39]. Since adjacent carboxylic acid functional groups are not coordinated to the metal center, they can serve as connection points to targeting vectors. The thermodynamic stability constant (log β_1) of 26.24 is high enough for radiopharmaceutical applications. Ligand PrP9 (**3g**) additionally exhibits selectivity for small cations similar to that of NOTA (**3**), while the constants of formation of complexes with Cu(II) and Zn(II) are 10 orders of magnitude lower than those of the corresponding complex Ga(III). The ^{68}Ga radiolabeling yields for PrP9 of over 95% were achieved within 5 min at 60°C in the pH range 1–5. The functionalization of carboxylic acid side chains did not significantly affect the labeling efficiency. A unique feature of PrP9 is the ability to give high labeling yields at very low pH.

Another phosphorylated analogue of NOTA, NOPO (Fig. 4a, **3h**) also exhibits exceptional selectivity to Ga(III), demonstrating a high proportion of gallium incorporation even in a medium containing a large quantity of other metal impurities [7]. In addition, this chelator is characterized by efficient complex formation even at room temperature and low concentrations (1–10 μM).

A derivative of phosphonic acid H_5NOA2P (**3i**) (1,4,7-triazacyclononane-*N*,*N*′-bis(methylenephosphonic acid)-*N*″-methylenecarboxylic acid) (Fig. 4a) belongs to the class of triazacyclic ligands. Its high binding constant with ^{69}Ga log β_1 = 34.44 surpasses NOTA (**3**) and DOTA (**1**). However, the radiolabeling of such a structure occurs quite slowly at 95°C for 30 min. The stability of this complex at pH 7.4 is somewhat higher than that of Ga(III) with transferrin. With regard to biological activity, it has been established that, despite the rather high stability of H_5NOA2P (**3i**) *in vivo*, it is quickly excreted from the body by the kidneys. Nevertheless, the possibility of more efficient binding to peptides or octreotide for similar structures containing two methylenephosphonic groups has been noted. This demonstrates the potential for a more detailed study of the bioconjugation of such complexes in living systems [8].

Hexadentate chelators based on 6-amino-1,4-diazepine triacetate (DATA, **4**) form octahedral complexes with Ga(III) (Fig. 5).

For all four chelators, the radiochemical yield was quite high for 10 min. For DATA^{Ph} (**4a**) and DATA^{M} (**4b**), they reached 97% and 93%; for DATAP^{Ph} (**4c**) and DATA^{Ph} (**4d**), the yields were 93% and 84% after 1 and 10 min, respectively. The fact that such complexes exist across a wide range of temperatures and pH (4–7) makes them quite labile and widely applicable for various bioconjugates, especially if they are sensitive to the conditions of the biological environment. The fairly wide spread of lipophilicity for all four complexes is also of great importance for individual distribution *in vivo*, allowing a chelator for the vector to be more accurately selected [10, 43, 44].

A macrocyclic chelator based on a chelating agent, which was developed two decades ago, has recently been tested for radiopharmaceutical purposes [45]. Ligand *p*-NO_2-Bn-PCTA (**5**) (PCTA (**5a**) = 3,6,9,15-tetraazabicyclo[9.3.1]pentadeca-1,11,13-triene-3,6,9-triacetic acid) (Fig. 6) is based

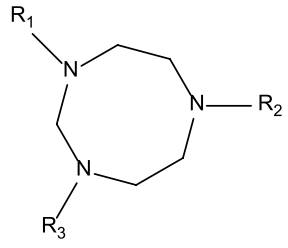

PrP9 (TRAP), **3g**: $R_1 = R_2 = R_3 = P(O)(OH)CH_2CH_2COOH$,
NOPO, **3h**: $R_1 = R_2 = CH_2P(O)(OH)CH_2OH$,
$R_3 = CH_2P(O)(OH)CH_2CH_2COOH$,
H_5NOA2P, **3i**: $R_1 = R_2 = P(O)(OH)_2$,
$R_3 = COOH$.

a

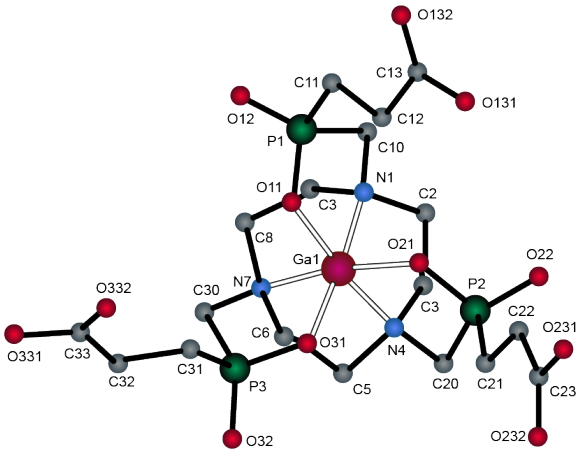

b

Fig. 4. (a) Structures of PrP9 TRAP (**3g**), NOPO (**3h**), and H_5NOA2P (**3i**);
(b) crystal structure of PrP9 (TRAP) (**3g**) with gallium [6].

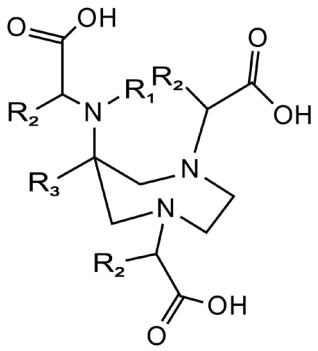

4

R_1 = H, $R_{2,3}$ = CH_3 $DATA^P$ (**4a**),
$R_{1,3}$ = CH_3, R_2 = H $DATA^M$ (**4b**),
R_1 = H, R_2 = CH_3, R_3 = Ph $DATA^{PPh}$ (**4c**),
$R_{1,2}$ = H, R_3 = Ph $DATA^{Ph}$ (**4d**)

Fig. 5. DATA (**4**) and its analogues.

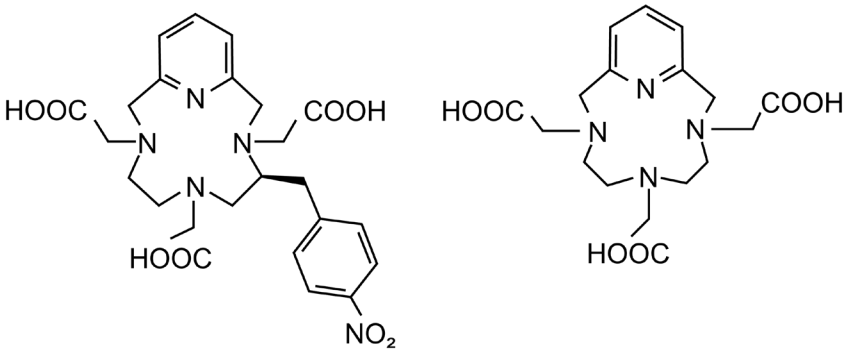

5 5a

Fig. 6. *p*-NO_2-Bn-PCTA (**5**).

on a 12-membered tetraaze macrocycle containing a pyridine group with a *p*-nitrobenzyl substituent, which can be converted to an isocyanide for attachment to a targeting vector [46].

The lower thermodynamic stability (log β_1 = 19.37) of complexes of PCTA (**5a**) with metals can be attributed to their lower overall basicity as compared with the corresponding DOTA (**1**) complexes. As a consequence, the competition between protons and metal ions for PCTA (**5a**) is lower than for DOTA (**1**), making PCTA (**5a**) the best ligand over the entire pH range. In addition, PCTA was found to have a much faster complexation than DOTA (**1**) [46]. The *p*-NO_2-Bn-PCTA ligand (**5**), which demonstrated higher labeling efficiency compared to *p*-NO_2-Bn-DOTA (**1a**), achieved a radiochemical yield of over 96% at pH 3 to 5 and room temperature.

The $^{67/68}$Ga-*p*-NO_2-Bn-PCTA complexes were highly kinetically stable with little degradation or loss of ^{67}Ga following incubation for 24 h at pH 2. In the presence of excess apotransferrin at 37°C, ^{68}Ga-*p*-NO_2-Bn-PCTA showed transchelation of approximately 10% to protein within 4 h.

Sarcophagin-type BFCs (sarcophagin = sar = 3,6,10,13,16,19-hexaazabicyclo[6.6.6]icosane) were originally developed for ^{64}Cu radiopharmaceuticals but have recently been evaluated for ^{68}Ga labeling (Fig. 7a).

Metal complexes of this chelator type are extremely stable due to the rigidity and encapsulating nature of the cell's amino ligand backbone. In the crystal structure of the Ga(III)-(1-NH_3-8-NH_2)-sar complex, the Ga(III) cation is six-coordinated with the N_6 donor in a trigonally distorted octahedral geometry [11].

For the conjugation of two cyclic RGD peptides to target the $\alpha_v\beta_3$ integrin receptor, a diamsar derivative with two glutamic acid residues conjugated to primary amino groups through amide bonds was studied [11]. In contrast to labeling with ^{64}Cu, which usually gives high yields at room temperature, for labeling the ^{68}Ga bioconjugate, the diamsar-RGD dimeric complex was heated at 85°C for 30 min. However, a quantitative labeling with a yield of more than 98% was achieved this way. The ^{68}Ga-labeled conjugate showed no transfer

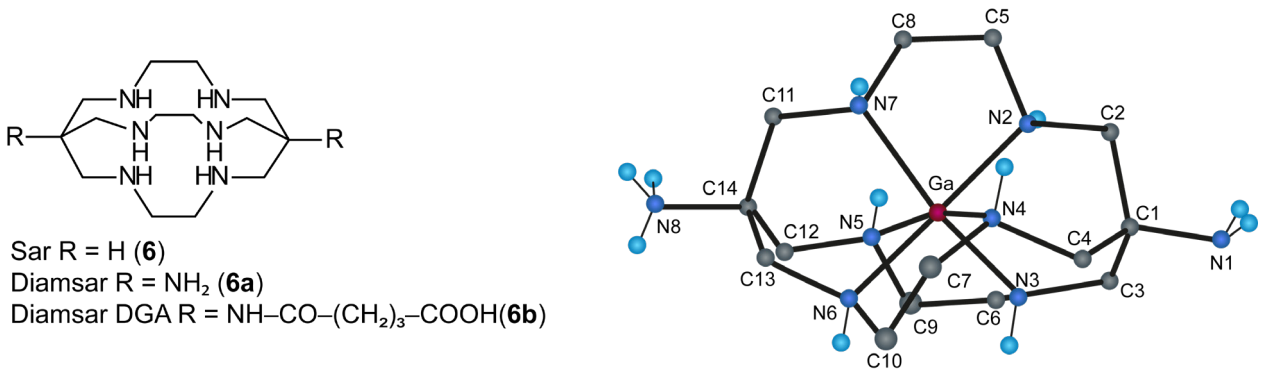

Fig. 7. (a) The sarcaphagin-type BFC structure, (b) X-ray diffraction analysis results of diamsar (**6a**) complex with gallium [11].

to apotransferrin for up to 2 h in an *in vitro* study, but showed specific binding to the receptor *in vitro* and demonstrated high selective tumor uptake with predominantly renal clearance in biodistribution and microPET imaging studies.

ACYCLIC CHELATORS

The macrocyclic effect generally results in kinetically more inert and thermodynamically more stable metal complexes of macrocyclic chelators compared to acyclic ligands, making macrocycle-based BFCs more attractive for radiopharmaceutical applications. However, the fairly successful *in vivo* acyclic chelators are superior to their macrocyclic counterparts. A significant advantage of acyclic ligands is their faster metal binding, which leads to faster radioactive labeling, especially in the case of shorter-lived radiometals such as ^{68}Ga [47, 48].

A representative ligand of this class is the acyclic chelator HBED (*N*,*N*′-bis-(2-hydroxybenzyl)-ethylenediamine-*N*,*N*′-diacetic acid) (**7**). Based on an EDTA-type framework with two hanging phenolic branches, this ligand has recently attracted increased attention in the development of BFC for radiopharmaceutical applications (Fig. 8) [14, 49].

When this ligand was developed in the 1950s, it was observed to form highly stable complexes with Ga(III) (log β_1 = 38.51) [13]. The acyclic bifunctional ligand HBED-CC (*N*,*N*′-bis-[2-hydroxy-5-(carboxyethyl)-benzyl]ethylene-diamine-*N*,*N*′-diacetic acid) (**7a**), which is characterized by rapid and efficient radioactive labeling at room temperature, has high *in vivo* stability; for this reason, it is used for labeling thermosensitive biomolecules [14, 15, 49]. An intact monoclonal antibody (mAb) used as a model protein with a recombinant diabody was consequentially linked to HBED-CC (**7a**) [49]. ^{68}Ga binding

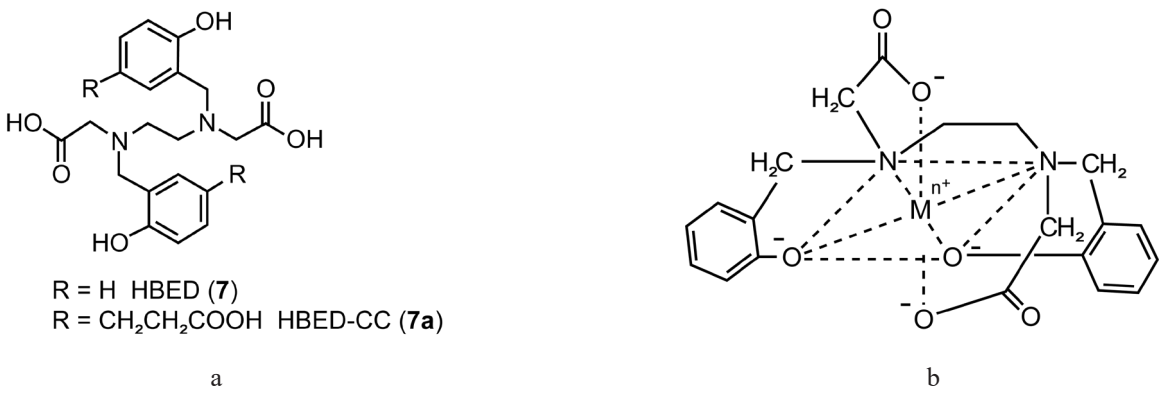

Fig. 8. (a) HBED (**7**) and HBED-CC (**7a**), (b) HBED complex (**7**) with gallium.

to the HBED-CC-mAb bioconjugate gave high radiochemical yields under mild conditions. Complexation at pH 4.1 for 5 min at 40°C produced a 89% yield of radiolabeled bioconjugate, as compared with diabody labeling, which achieved a slightly lower yield of 85% in a HEPES buffer at pH 4.5 and 40°C. Binding assays showed that labeled ^{68}Ga-HBED-CC did not significantly affect the receptor binding of the antibody and the diabody. In addition, the acyclic BFC HBED-CC (**7a**) was evaluated in a second comparative study with NOTA (**7a**) [14]. HBED-CC (**7a**) was conjugated to protein via activated *N*-hydroxysuccinimide. The protein used in this study was single chain vascular endothelial growth factor (VEGF) expressed with a cysteine containing fusion tag (Cys-tag) for site-specific conjugation of PEGylated bifunctional chelating agents. The corresponding bioconjugates HBED-CC (**7a**) and NOTA (**3**) were labeled at pH 4.2 and room temperature. Under these conditions, the HBED-CC conjugate (**7a**) bound quantitatively (98.7%) within 4 min, while the binding to NOTA (**3**) was 50%. To achieve a comparable labeling result for NOTA (**3**), an incubation of more than 10 min was required.

The HBED-CC (**7a**) and NOTA (**3**) conjugates were highly stable, as it was demonstrated by a long-term radiochemical study of human serum, in which no decomplexation was observed after 72 h. In cell-to-cell binding studies with 293/KDR cells, both radiolabelled bioconjugates showed comparable binding with nearly identical K_D values (0.67 for HBED-CC (**7a**) vs. 0.59 for NOTA (**3**)), which are in excellent agreement with other radiolabeled scVEGF tracers. Biodistribution studies of both indicators using *ex vivo* imaging and PET in mice with tumor showed a similar distribution pattern for both indicators, however, liver uptake of the HBED-CC conjugate (**7a**) was markedly lower than for the NOTA analogue (**3**). On the other hand, the renal uptake of NOTA (**3**) was lower compared to HBED-CC (**7a**).

A possible modification of HBED-CC (**7a**) at propionic acid residues led to the creation of mono- and bis-condensation products with 4-amino-*N*-(4-((3-bromophenyl)amino)quinazolin-6-yl) butanamide. MTT analysis of mono- and bis-condensed products and their corresponding complexes showed IC_{50} values below 70 μM in the A431 cancer cell line, making them the first complexes of Ga(III) with quinazoline derivatives demonstrating antiproliferative activity in the micromolar range described in literature. Previous studies of quinazoline analogues coupled to the DOTA (**1**) chelator and labeled with ^{67}Ga did not show any cytotoxicity even at higher concentrations [15].

Pyridine chelators are actively developed, one of the best examples being H2dedpa (**8**) (6,6'-(ethane-1,2-diylbis(azandiylbis(methylene) dipicolinic acid) (R = H) and its corresponding precursor (R = 1-methyl-4 nitrobenzene) (**8a**) (Fig. 9), which also belong to acyclic chelators [12].

The H_2dedpa (**8**) ligand binds Ga(III) in a distorted octahedral manner with two carboxylate donor atoms, two pyridine ring nitrogens, and two secondary amine N-donor atoms both in solution and in the solid state, and forms Ga(III) complexes with a high thermodynamic stability (log β_1 = 28.11). The coupling of H_2dedpa (**8**) and its ^{68}Ga bioconjugate precursor gave quantitative yields within 10 min at room temperature. Once formed, the complex remains intact up to 97% for 2 h in an *in vitro* transferrin challenge experiment.

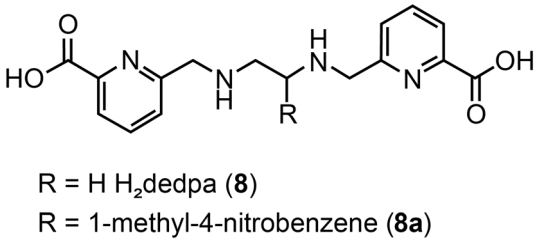

R = H H_2dedpa (**8**)
R = 1-methyl-4-nitrobenzene (**8a**)

a

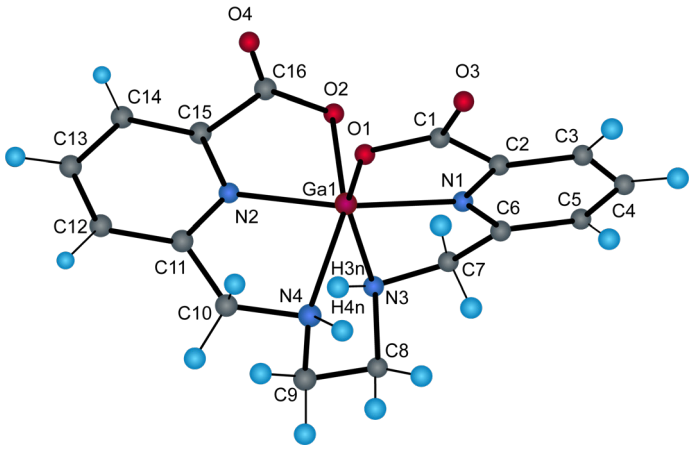

b

Fig. 9. (a) H_2dedpa structure (**8**), (b) a crystal structure of H_2dedpa with gallium [12].

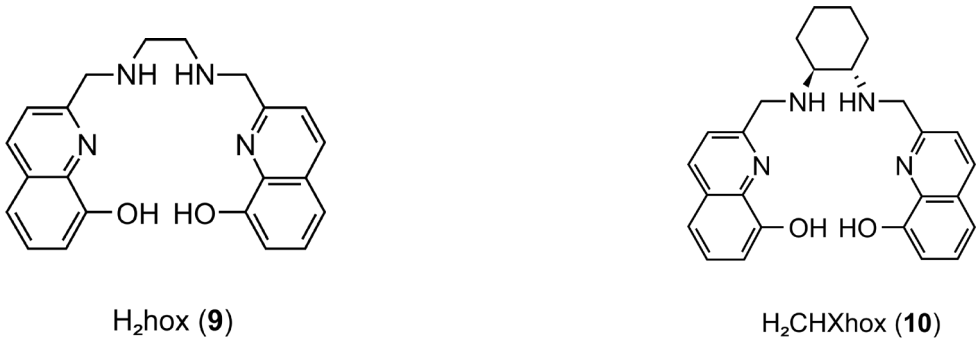

Fig. 10. Structural formulas of H_2hox (**9**) and H_2CHXhox (**10**).

Increasing the degree of preorganization by adding a *trans*-1,2-cyclohexanediamine backbone, such as in H_2hox (**9**) and H_2CHXhox (**10**), results in an increase in the kinetic inertness of the complex (Fig. 10). This modification also resulted in a higher thermodynamic stability of [^{nat}Ga]H_2CHXhox compared to [^{nat}Ga]H_2hox, and a superior stability of [^{nat}Ga]H_2CHXhox at pH 1. Radiolabeling of both H_2hox (**9**) (5 min, 25°C, $1\cdot10^{-7}$ M, pH 8.5), and H_2CHXhox (**10**) (~1 min, Δ, $2.1\cdot10^{-5}$ M, pH 5) with ^{68}Ga chloride proceeded in a short period of time and showed good *in vivo* stability along with limited toxicity *in vitro*. Due to milder radiolabeling conditions, these chelators are promising candidates as BFC for biological vectors [35].

Tris(8-quinolinolate) gallium(III) (KP46) (**11**) has been developed to provide high oral bioavailability of gallium during cancer treatment. In contrast to gallium(III) chloride, KP46 (**11**) shows higher cellular uptake in rat glioblastoma cells, causing a significant decrease in intracellular levels of deoxyribonucleoside triphosphate [16].

KP46 (**11**) is 10 times more active against A549 human lung malignant adenocarcinoma cells than gallium chloride, which exhibited dose- and time-dependent cytotoxicity, while KP46 (**11**) cytotoxic activity was dose-dependent only. These results suggested that the mechanisms of action of gallium chloride and KP46 (**11**) are different [50]. To evaluate the safety, toxicity profile and pharmacokinetics of the drug, a phase I trial of KP46 (**11**) was conducted in 2004. Seven patients with advanced malignant solid tumors located in the kidney, ovary, stomach, and parotid gland were treated with KP46 (**11**). Oral administration of KP46 (**11**) was effective in three out of four patients with renal cell carcinoma. Studies have shown that a long terminal half-life, high total clearance, and a large apparent volume of distribution characterize the pharmacokinetics of gallium [16, 51].

Its analogue, 5-chloro-8-quinolinol (**12**), can also form a tris-coordinated structure, where nitrogen and oxygen atoms coordinate the gallium atom (Fig. 11).

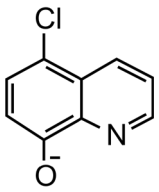

12

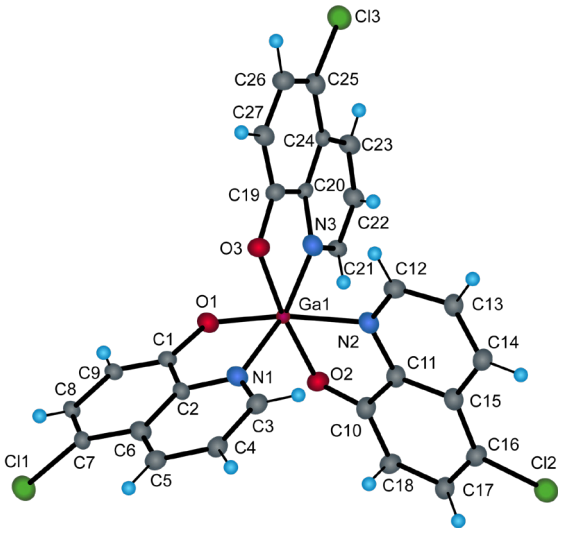

Fig. 11. (a) 5-Chloro-8-quinolinone (**12**), (b) its crystal structure with gallium [52].

This complex was tested for cytotoxicity against A2780 ovarian cancer cells, MDA-MB-231 breast carcinoma (derived from a metastasis site), HCT116 epithelial colorectal cancer cell line, and MRC5pd30 non-cancerous human lung tissue cells. The complex showed good activity against a whole panel of cancer cell lines with IC_{50} values in the low micromolar concentration range. It exhibited potency comparable to clinically used cisplatin in cisplatin-responsive A2780 cells, but was significantly more active in cisplatin-initially resistant colon and breast cancer cells, including the difficult-to-treat, highly metastatic MDA-MB-231 cell line. In addition, it showed a clear selectivity for malignant tumor cells compared to benign lung fibroblastoma (MRC5pd30) [52].

Dimethoxypyridine-3-carboxylic acid is also capable of complexing with Ga^tBu_3—$[Ga^tBu_2(\mu\text{-DMP-kO:kO'})]_2$ (**13**), forming a tetracoordinate structure with a distorted tetrahedral configuration, with two *tert*-butyl groups and two different oxygen atoms of two different metal-bound carboxylate ligands (Fig. 12).

The *in vitro* cytotoxicity of $[Ga^tBu_2(\mu\text{-DMP-kO:kO'})]_2$ (**13**) against the HeLa human adenocarcinoma, Fem-x human malignant melanoma, K562 human myelogenous leukemia, and MDA-MB-361 human breast carcinoma showed a dose-dependent antiproliferative effect. The complex has a higher cytotoxic activity against K562 compared to other cell lines, indicating some preferential activity under these conditions [53].

In a series of ligands based on 3-hydroxy-4-pyridinone (GPO), the hexadentate chelator CP256 (R = acyl) (**14a**) and its bifunctional version YM103 (R = *N*-(3-amino-3-oxopropyl)-3-(2,5-dioxo-2,5-dihydro-1H-pyrrol-1-yl)propane) (**14b**) showed a very high labeling efficiency at room temperature with a radiochemical yield of more than 98% within 5 min at pH 6.5 (Fig. 13) [18].

In studies of the stability of the ^{68}Ga-CP256 complex in human serum under control infection with apotransferrin, neither decomplexation nor transchelation was observed, which indicates its high stability and inertness. PET imaging studies using the C2Ac protein as a target vector, which is analogous to the phosphatidylserine-binding domain of synaptotagmin I, further confirmed stability *in vivo*.

Another chelator based on hexadentate GPO, $NTP(PrHP)_3$ (**14c**), is used as a metal-binding agent for chelation therapy and may be suitable for labeling ^{68}Ga biomolecules (Fig. 14) [54, 55]. The $NTP(PrHP)_3$ ligand (**14c**) forms a hexacoordinate complex with Ga(III) with high thermodynamic stability (log β_1 = 33.34), however, it has been shown in titration experiments that at pH > 6 it changes to a water-insoluble form, what should be explicitly avoided in radiopharmaceutical applications. However, the therapeutic concentrations at which this drug can be used are an order of magnitude lower than the concentrations that have a significant effect on its solubility.

The radiochemical purity of the ^{67}Ga-$NTP(PrHP)_3$ complex was more than 98%. Due to the ability of $NTP(PrHP)_3$ (**14c**) to coordinate ^{67}Ga *in vivo*, its activity was investigated by co-administration

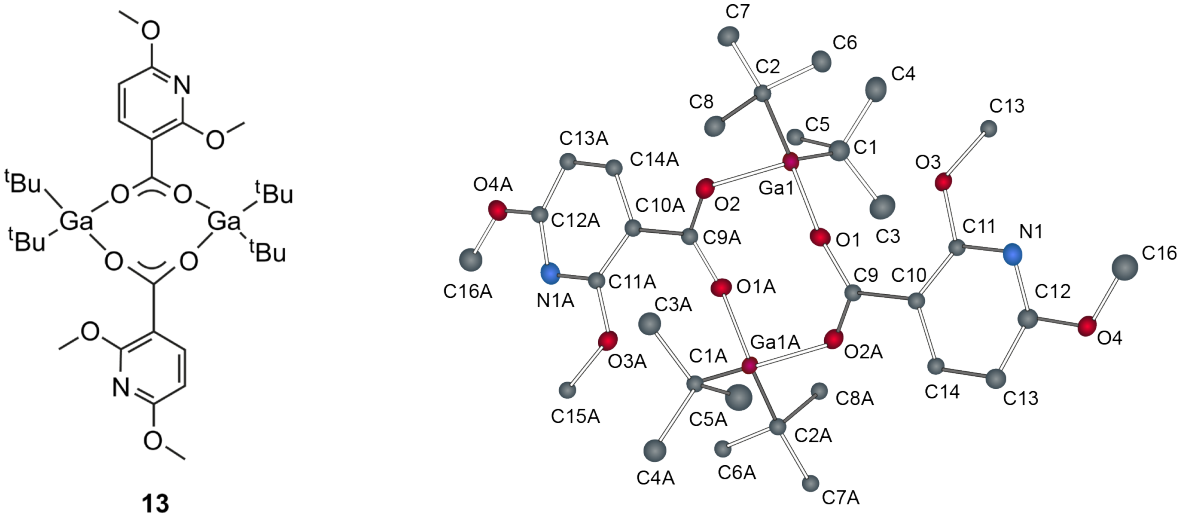

Fig. 12. (a) $[Ga^tBu_2(\mu\text{-DMP-kO:kO'})]_2$ (**13**), (b) its crystal structure with Ga^tBu_2 [53].

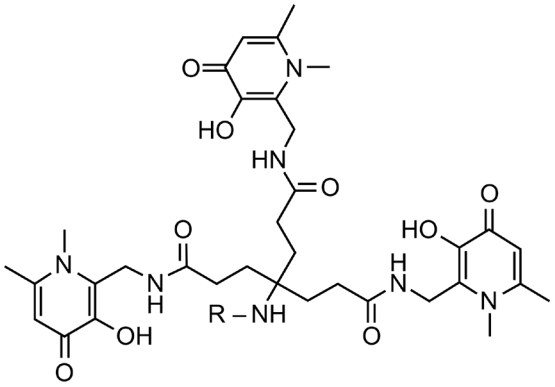

R = H DPO (**14**),
R = acyl CP256 (**14a**),
R = *N*-(3-amino-3-oxopropyl)-3-(2,5-dioxo-2,5-dihydro-1H-pyrrol-1-yl)propane YM103 (**14b**).

Fig. 13. DPO (**14**), CP256 (**14a**), and YM103 (**14b**).

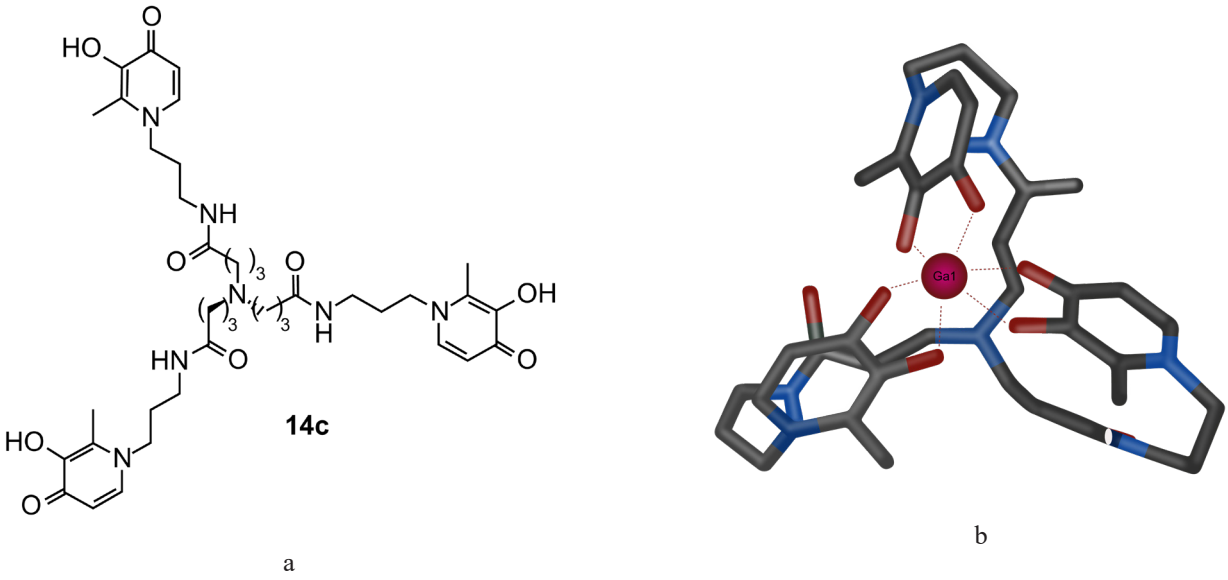

a b

Fig. 14. (a) Structure of NTP(PrHP)$_3$ (**14c**), (b) XRD results of its complex with gallium [54].

of the ligand after injection of ^{67}Ga-citrate, which causes a rapid clearance of ^{67}Ga from blood, muscles, and bones. In an additional biodistribution study of the ^{67}Ga-NTP(PrHP)$_3$ complex, no significant differences in uptake and clearance were noted. A study of the ^{67}Ga-NTP(PrHP)$_3$ complex, carried out on Wistar rats, showed that it was mainly localized in the blood, kidneys, and liver after 30 and 60 min with little or no absorption by other organs. ^{67}Ga-NTP(PrHP)$_3$ was rapidly cleared from the blood and only 2% of the administered dose was present after 60 min. After 24 h, the complex was largely eliminated from all tissues, with the exception of the kidneys, where about 10% of the original concentration was still present.

The deferoxamine (DFO) chelator (**15**) is well known for its use in iron chelation therapy (Fig. 15). The similarity of high-spin Fe(III) with Ga(III) determines the ability of DFO (**15**) to form complexes with Ga(III), which also have high thermodynamic stability. The possibility of its use as a BFC for gallium radioisotopes has been proven in combination with peptides and small molecules [20, 56, 57].

^{67}Ga labeling was effective, but the complex was poorly retained in cells after antibody

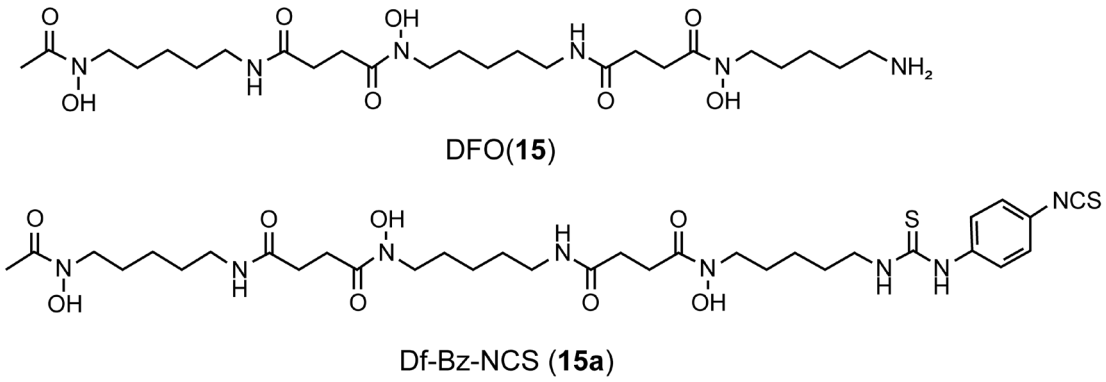

Fig. 15. DFO (**15**) and Df-Bz-NCS (**15a**).

internalization and, probably, after biotransformation. Van Dongen *et al*. have addressed this issue: he used BFC Df-Bz-NCS (*p*-isothiocyanatobenzyl-desferrioxamine) (**15a**), which was conjugated with the 7D12 nanobody against the epidermal growth factor receptor (EGFR) (Fig. 15) [21]. $^{68/67}$Ga labeling was achieved by incubating the Df-bioconjugate at pH 7.2 for 5 min, followed by column purification. The $^{68/67}$Ga-Df-Bz-NCS-7D12 conjugate was stable in human serum with a radioactivity loss of less than 2% at 2 h and 7% at 24 h. In biodistribution studies, ^{68}Ga labeled 7D12 nanobody showed high uptake in A431 tumors. There was no significant accumulation in other organs, with the exception of the kidneys. In PET imaging studies, the tumor was clearly visualized using ^{68}Ga-Df-Bz-NCS-7D12.

Bispidines (compounds based on the core of 3,7-diazabicyclo[3.3.1]nonane) (**16**) are widely used chelators with a well-organized coordination site (Fig. 16). They have been used to form complexes with a range of metals, including radioactive ones such as copper-64, whose complexes have proven to be extremely inert. However, the use of bispidines for the chelationof Ga(III) and, in particular, ^{68}Ga, remained relatively unexplored until recently [58].

Bispidine ligand (**16**) was first used for complex formation with Ga(III) and was labeled with ^{68}Ga. Despite its 5-coordinate nature, the resulting complex is stable in serum for more than 2 h, showing a ligand system well matched to the imaging window of ^{68}Ga PET. To show the versatility of the bispidine ligand (**16**) and its potential use in PET, a bifunctional chelator was conjugated to a porphyrin. The resulting compound showed the same level of serum stability as the unconjugated ^{68}Ga complex.

The complexation of Ga(III) with bispidine (**16**) was carried out at pH 4–4.5 and reflux. A radiochemical yield of 89% was achieved at a ligand concentration of 100 μM, while at 200 μM the yield was 94% (Fig. 17).

In terms of complexation kinetics and radiolabeling efficiency, bispidine (**16**) is not as effective as NOTA (**3**) and the phosphine analogue TRAP (**3g**), which can be labeled with a radioactive

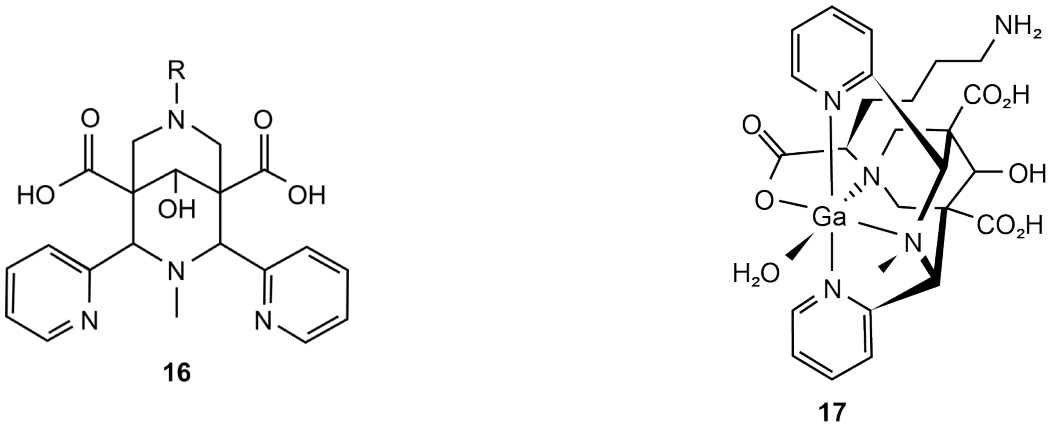

a b

Fig. 16. (a) Bispidine (**16**), (b) complex of bispidine with gallium (**17**) [58].

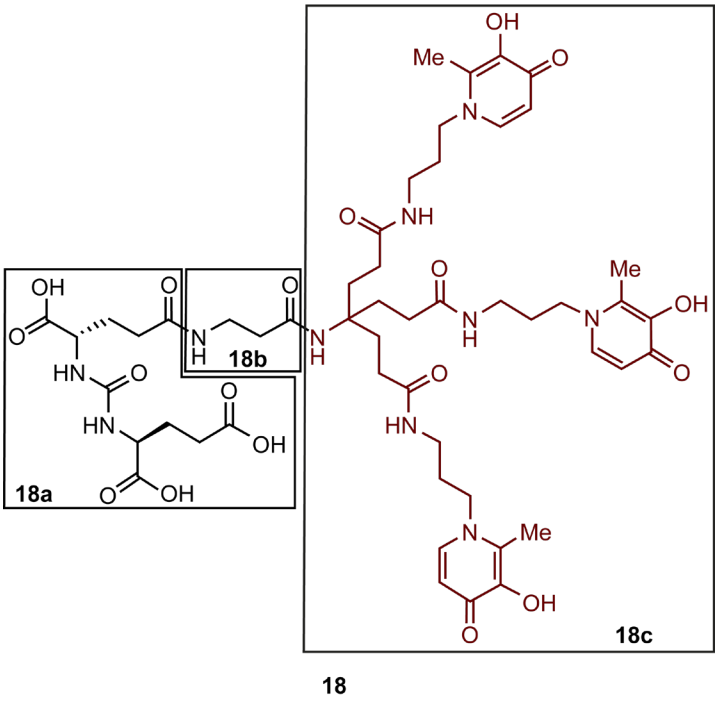

18

Fig. 17. DUPA-β-Ala-KC18 (**18**).

isotope at much lower concentrations at 95°C or at room temperature using large excess of ligand. A similar trend is observed when compared with acyclic ligands such as H_2dedpa (**8**) and H_3dpa (**8b**). These differences are not surprising, since bispidine is a pentadentate ligand, which is not optimal for Ga(III) complexation in terms of kinetics, selectivity, and thermodynamic stability.

However, based on observations of the behavior of analogous ^{64}Cu compounds, one can expect positive results in terms of kinetic inertness when using a bispidine framework. When evaluating radiochemical stability, decomplexation was not observed for 2 h at 37°C, which proves the suitability of this ligand for ^{68}Ga-PET *in vivo*. In addition, it is contemplated that radiochemical yields and radiolabeling conditions can be further improved by using other bispidine derivatives, in particular those with a hexadentate coordination site [58].

A recently emerging class of chelators is based on tris-(hydroxypyridinone) (THP) (**17**). THP-peptide bioconjugates complex with ^{68}Ga rapidly and quantitatively at room temperature, neutral pH, and micromolar ligand concentrations, which makes them suitable for the synthesis of PET radiopharmaceuticals. A bifunctional chelator named THP-PSMA (**17a**) represents this class of compounds. In THPPSMA (**17a**) there are three groups of 1,6 dimethyl-3-hydroxy-4-pyridinone and glutamate-urea-lysine. In additionto the aforementioned advantages, the chelation process with this ^{68}Ga ligand is not affected by the presence of other metal ions such as Fe^{3+}. However, ^{68}Ga-THP-PSMA showed lower absolute tumor uptake compared to ^{68}Ga-PSMA-11 [59].

For this reason, a new conjugate was synthesized containing 3-hydroxypyridin-4-one (**17**) and a fragment of DUPA (**18a**) (2-[3-(1,3-dicarboxypropyl)-ureido]-pentanedioic acid), called DUPA-β-Ala-KC18 (Fig. 17). In DUPA-β-Ala-KC18 (**18**), DUPA (**18a**) acts as a PSMA (prostate specific membrane antigen) targeting moiety and KC18 (**18c**) acts as a Ga(III) chelating moiety; β-Ala (**18b**) was used as a linker to separate the sefragments. The performed studies have found that DUPA-β-Ala-KC18 (**18**) can quickly form a stable complex with $^{nat}Ga^{3+}$, which implies that DUPA-β-Ala-KC18 (**18**) can be efficiently labeled with ^{68}Ga [60].

Another promising class of ligands for gallium are thiosemicarbazone derivatives, which have potentially high antitumor activity. It was shown that thiosemicarbazones in complex with Ga(III) inhibit the activity of ribonucleoside diphosphate reductase (RDR) and have antiproliferative properties. Due to its similarity to Fe(III), Ga(III) affects the availability of intracellular iron, but also interacts directly with RDR by competing with iron for its binding site in the R2 subunit of the enzyme. The combination of the central metal and ligand, which are directed to the same molecular target using different mechanisms of action, can constitute a strategy for obtaining potent RDR inhibitors in which the two structural components exhibit a synergistic effect [61].

The reaction of 2-acetylpyridine ^{4}*N*-dimethylthiosemicarbazone with $GaCl_3$ leads to the formation of the complex $[GaL_2][GaCl_4]$ (KP1089) (Fig. 18). The gallium atom in this compound is coordinated with two nearly planar tridentate ligands. The coordination polyhedron approaches an octahedron, where two ligands are bonded to the gallium atom through the nitrogen atom of the pyridine ring, the nitrogen atom, and the sulfur atom of thiosemicarbazide [62]. The complex was tested for cytotoxicity against human tumor cell lines SW480 (colon adenoma), SK-BR-3 (breast adenocarcinoma), and 41M (ovarian carcinoma) [62].

$[GaL_2][GaCl_4]$ had a strong antiproliferative effect at nanomolar concentrations in 41M, SK-BR-3, and SW480 cells, and the cytotoxicity of the complex was slightly higher against 41M cells than for free thiosemicarbazone. Similar results were obtained with SK-BR-3 and SW480 cells.

Alkylthiosemicarbazones (**20a-d**) (Fig. 19a) modified at the N4 position and their complexes with metals also exhibit significant anticancer

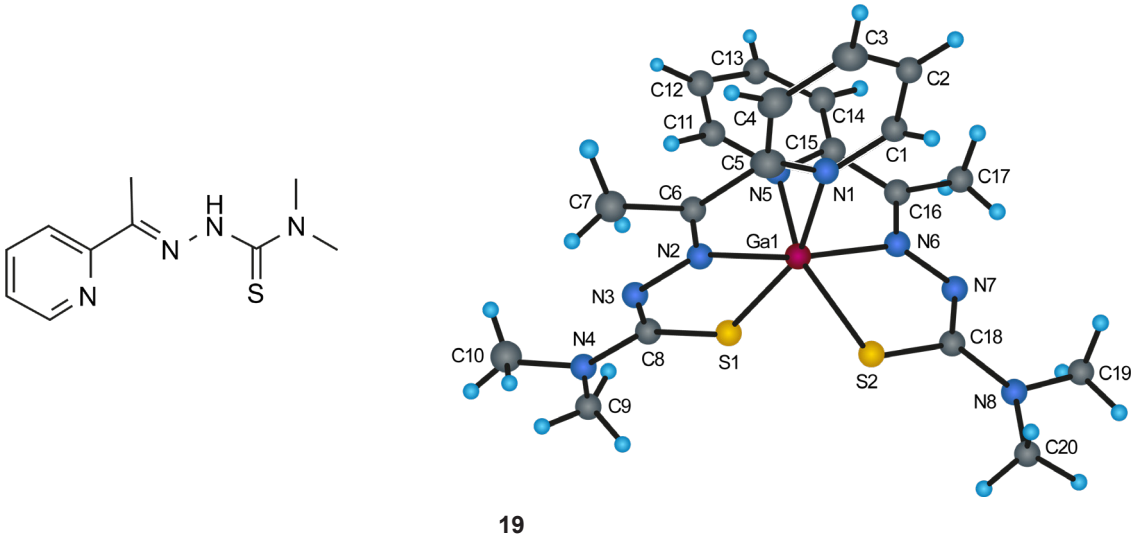

Fig. 18. (a) 2-acetylpyridine ^{4}*N*-dimethylthiosemicarbazone (**19**) structure, (b) crystal structure of $[GaL_2][GaCl_4]$ [62].

activity. Upon modification of the methyl, phenyl, and pyridyl groups at the R_1 position of α-*N*-heterocyclic piperidylthiosemicarbazones, the activity increases consistently. For α-*N*-heterocyclic piperidylthiosemicarbazones (**21a-c**) (Fig. 19b), a decrease in activity is observed upon modification of the R_2 substituent in the H → methyl → ethyl series at the position of the pyrazine fragment.

It is also important to note that α-*N*-heterocyclic piperidylthiosemicarbazones (**21a-c**) and their complexes with gallium exhibit low toxicity (IC_{50} > 30 μm) towards normal cells (MRC-5).

The results of a study of cellular Ga uptake performed on the MCF-7 cell line showed that complexes of thiosemicarbazone ligands with gallium are easily absorbed by cells and thus have a potentially high bioavailability. Regarding the mechanism of anticancer activity, it was found that these complexes have the ability to increase the expression of the transferrin-1 receptor (TfR1) and at the same time to suppress the expression of ferritin, which leads, on the one hand, to an increase in the intracellular concentration of iron and, on the other hand, to a decrease in the possibility of its deposition and causes toxic effects. In addition, complexes of thiosemicarbazone ligands with gallium showed a rather high ability to activate apoptosis by acting simultaneously on several proteins involved in the mechanism of its intracellular activation. It was shown that both the parent thiosemicarbazone ligands and, to a greater extent, their complexes with gallium, are able to increase the expression of caspases-3, -7 and -9, along with an increase in the expression of cytochrome c (cyt-c) and apoptotic protease activating factor-1 (apaf-1), which together cause irreversible cell apoptosis. These experimental results indicate a great potential for using Ga(III) complexes with thiosemicarbazone ligands as effective anticancer drugs [63, 64].

2-Acetylpyridine- and 2-pyridinformamidiso nicotinoylhydrazones HAPIH (**22**) and HPAmIH (**23**) form a complex with Ga(III) in the form of a zwitterion (Fig. 20). The hexadentate structure is formed due to the coordination of Ga(III) with the nitrogens of the pyridinium rings, free hydroxyls and nitrogens of the enamine fragment, thereby forming a zwitterionic structure.

HAPIH (**22**) and HPAmIH (**23**) were tested against HL-60 (leukemia), MCF-7 (breast cancer), HCT-116 (colorectal cancer), PC3 (prostate cancer) and HEK-293 (non-malignant human embryonic kidney cells). HAPIH (**22**) was most cytotoxic against colorectal cancer cells IC_{50} = 1.6 μM. Also, for HEK-293, both ligands turned out to be 25 times less toxic compared to other cells of malignant neoplasms [65].

The 2-acetylpyridine-7-isoquinoline thiosemicarbazone analogue (**24**) (Fig. 21) proved to be quite effective in complex with Ga(III) as an antimalarial drug against *P. falciparum*.

In addition, this complex was thirty-one times more active against HCT-116 cells (carcinoma), four times more effective against Caco-2 (adenocarcinoma) and two and a half times more effective against HT-29 (adenocarcinoma) by comparison with etoposide after 72 h. The complex was found

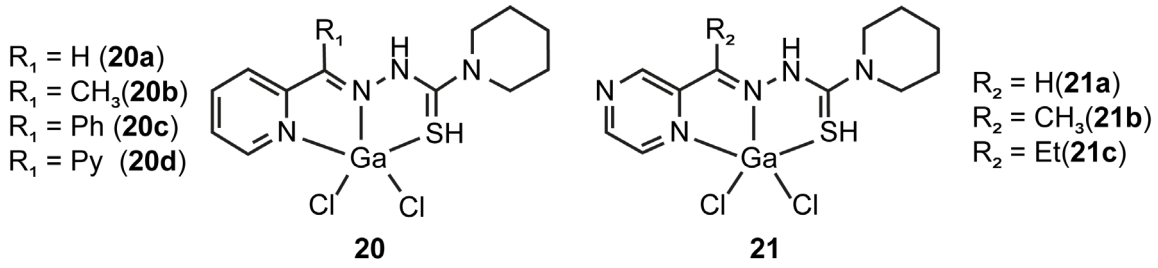

a b

Fig. 19. (a) Structures of complexes of alkylthiosemicarbazones (**20**),
(b) structures of complexes of piperidylthiosemicarbazones with gallium chloride (**21**).

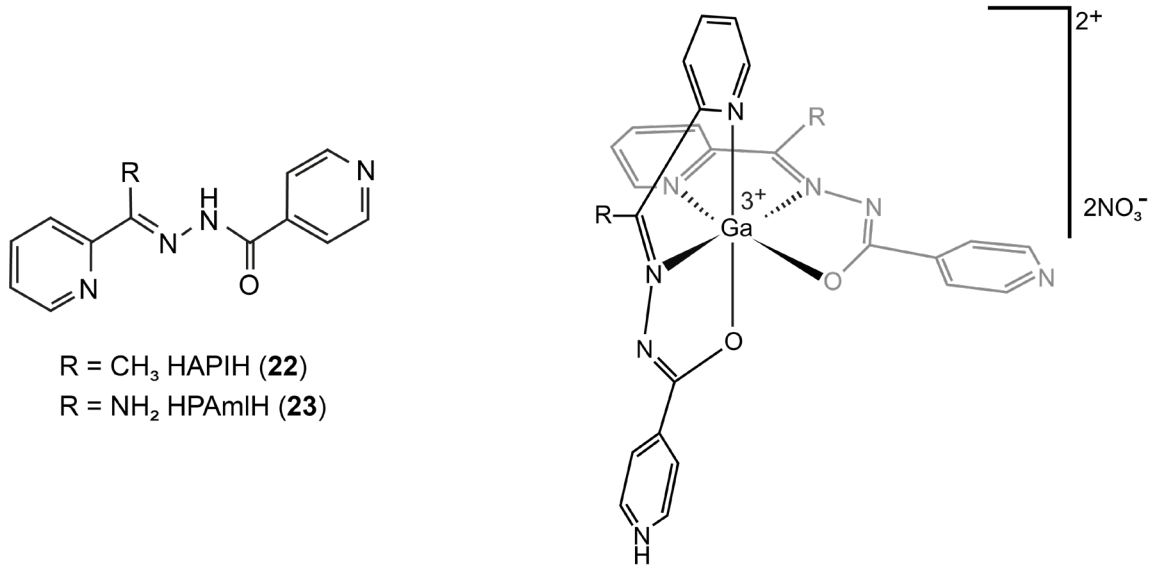

a b

Fig. 20. (a) Structure of HAPIH (**22**) and HPAmIH (**23**), (b) their complexes with gallium nitrate [65].

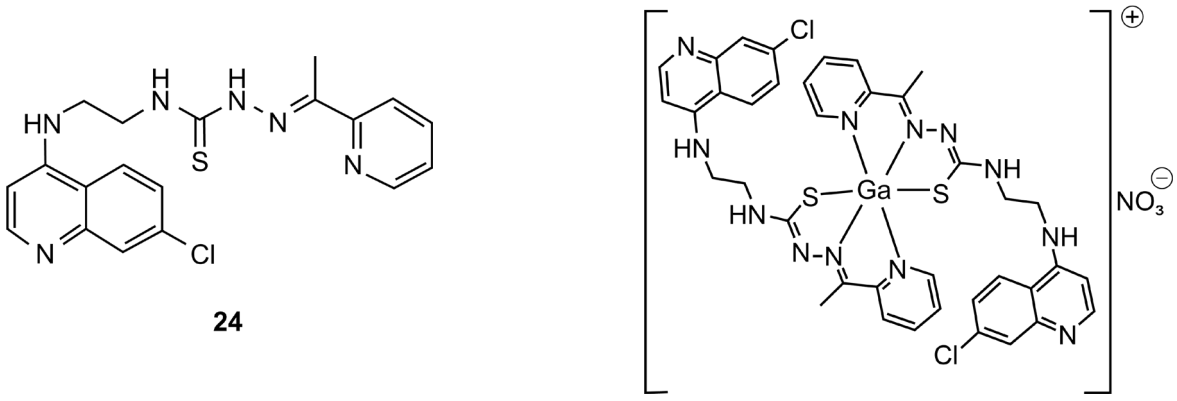

a b

Fig. 21. (a) *N*-(2-((7-chloroquinolin-4-yl)amino)ethyl)-2-(1-(pyridin-2-yl)ethylidene) hydrazinecarbothioamide (**24**),
(b) its complex with gallium nitrate.

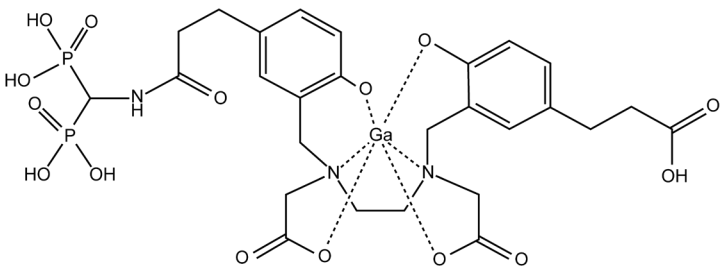

25

Fig. 22. Chemical structure of methylene diphosphonate [^{68}Ga]Ga-P15-041 (**25**).

to be non-cytotoxic compared to the benign colonic fibroblast cell line (CCD-18Co), showing IC_{50} = 11.81 ± 1.42 mM after 72 h [66].

In one of the latest studies of BFC to gallium, metastatic foci of prostate cancer were successfully visualized using [^{68}Ga]Ga-P15-041 (**25**) (Fig. 22), with the absorption in the lesion constantly exceeding the background.

Dynamic image analysis of [^{68}Ga]Ga-P15-041 uptake shows signal improvement relative to constant background over time for tumors with the highest uptake, but signal-to-noise ratio analysis shows that imaging is optimal between 60 and 90 min post-injection. Dynamic and dosimetric analyses show that [^{68}Ga]Ga-P15-041-PET imaging of prostate bone metastases in humans is possible, but further studies are needed to refine the initial results [67].

CONCLUSIONS

Over the past decades, tremendous progress has been made in the development of metal-based radiopharmaceuticals for PET, facilitating their use in the early detection of diseases. Significant progress has also been made in the development of bifunctional ^{68}Ga chelators that reliably bind the corresponding metal center *in vivo*. However, new BFCs should be developed with caution, as increased stringency can reduce labeling kinetics; therefore, higher temperatures and longer reaction times are required to achieve sufficient labeling yields. In addition to macrocyclic BFC, *in vivo* stable ^{68}Ga complexes formed with acyclic chelators have the advantage of faster labeling kinetics, which is a key factor given the short half-life of ^{68}Ga. Despite the significant progress, the problem of correlating the chemical structure of metal-based radiopharma ceuticals with their behavior *in vivo* remains to be solved. In this respect, comparative studies of drugs that have an identical targeting vector but include different BFCs may help further reveal the effect of the metal chelate moiety on pharmacokinetics. At the same time, the choice of the BFC's chelating fragment depends on the nature and degree of oxidation of the radiometal. There are many examples in literature showing that the nature of the BFC metal complex (geometry, lipophilicity, and total charge) plays a key role in determining the biodistribution of target radiopharmaceuticals.

Today, the main goal in the development of metal-based radiopharmaceuticals is the selection of effective bifunctional chelating agents, whose system forms a radiometal chelate with high thermodynamic stability and kinetic inertness to maintain the label on the targeting vector. The accumulation of radiometal in non-target tissues should not only be minimized in order to enhance image contrast, but also to minimize patients' exposure to radiation, which is particularly important in the case of radiotherapy applications.

Efficient and quantitative radioactive labeling eases the introduction of new indicators into clinical practice, allowing the preparation of radiopharmaceuticals without the need for additional purification.

Another important step for clinical translation is the selection of BFC to adjust the polarity and charge of the entire conjugate as a means of optimizing the clearance pathway and pharmacokinetics. For example, the clearance of a radiopharmaceutical from the blood should be slow enough to ensure optimal delivery to the target site, but at the same time rapid enough to avoid unnecessary radiation exposure. Thus, in order to create a BFC with high stability, efficient radioactive labeling kinetics and favorable pharmacokinetics is required along with a deep understanding of the radiometal coordination chemistry.

Acknowledgments

The presented work was supported by the Ministry of Science and Higher Education of the Russian Federation within the framework of the state task (project FSSM-2020-0004) "Development of the basics for obtaining and studying the interaction with the body of new multifunctional nanosized macromolecular systems for the targeted delivery of drugs, diagnostics and radiopharmaceuticals to combat the main socially significant diseases, including theranostics."

Authors' contributions

A.G. Polivanova – review of publications on the topic of the article, writing the text of the article, scientific editing;

I.N. Solovieva – review of publications on the topic of the article, writing the text of the article, analysis and systematization of the material;

D.O. Botev – review of publications on the topic of the article, writing the text, technical editing;

D.Y. Yuriev – review of publications on the topic of the article, technical editing, bibliography design;

A.N. Mylnikova – review of publications on the topic of the article, writing the text;

M.S. Oshchepkov – scientific editing, critical revision with valuable intellectual content.

The authors declare no conflicts of interest.

REFERENCES

1. Bartholomä M. Recent developments in the design of bifunctional chelators for metal-based radiopharmaceuticals used in Positron Emission Tomography. *Inorganica Chim. Acta*. 2012;389:36–51. https://doi.org/10.1016/j.ica.2012.01.061

2. Clarke E.T., Martell A.E. Stabilities of trivalent metal ion complexes of the tetraacetate derivatives of 12-, 13- and 14-membered tetraazamacrocycles. *Inorganica Chim. Acta.* 1991;190(1):37–46. https://doi.org/10.1016/S0020-1693(00)80229-7

3. Clarke E.T., Martell A.E. Stabilities of the Fe(III), Ga(III) and In(III) chelates of *N*,*N*′,*N*″-triazacyclononanetriacetic acid. *Inorganica Chim. Acta.* 1991;181(2):273–280. https://doi.org/10.1016/S0020-1693(00)86821-8

4. Velikyan I., Beyer G.J., Bergstrom-Pettermann E. The importance of high specific radioactivity in the performance of ^{68}Ga-labeled peptide. *Nucl. Med. Biol*. 2008;35(5):529–536. https://doi.org/10.1016/j.nucmedbio.2008.03.002

5. Riss P.J., *et al.* NODAPA-OH and NODAPA-$(NCS)_n$: Synthesis, ^{68}Ga-radiolabelling and *in vitro* characterisation of novel versatile bifunctional chelators for molecular imaging. *Bioorg. Med. Chem. Lett.* 2008;18(2):5364–5367. https://doi.org/10.1016/j.bmcl.2008.09.054

6. Notni J., Hermann P., Havlíčková J., *et al*. A Triazacyclononane-Based Bifunctional Phosphinate Ligand for the Preparation of Multimeric ^{68}Ga Tracers for Positron Emission Tomography. *Chem. Eur. J.* 2010;16(24):7174–7185. https://doi.org/10.1002/chem.200903281

7. Simeček J., *et al*. A monoreactive bifunctional triazacyclononane phosphinate chelator with high selectivity for gallium-68. *ChemMedChem*. 2012;8(7):1375–1378. https://doi.org/10.1002/cmdc.201200261

8. Prata M.I.M., *et al*. Gallium(III) chelates of mixed phosphonate-carboxylate triazamacrocyclic ligands relevant to nuclear medicine: Structural, stability and *in vivo* studies. *J. Inorg. Biochem*. 2017;177:8–16. https://doi.org/10.1016/j.jinorgbio.2017.08.015

9. Yang C.-T., Sreerama S.G., Hsieh W.-Y. Synthesis and Characterization of a Novel Macrocyclic Chelator with 3-Hydroxy-4-Pyrone Chelating Arms and Its Complexes with Medicinally Important Metals. *Inorg. Chem.* 2008;47(7):2719–2727. https://doi.org/10.1021/ic7022506

10. Seemann J., Waldron B.P., Roesch F. Approaching 'Kit-Type' Labelling with ^{68}Ga: The DATA Chelators. *ChemMedChem.* 2015;10(6):1019–1026. https://doi.org/10.1002/cmdc.201500092

11. Ma M.T., Neels O.C., Denoyer D., Roselt P., *et al*. Gallium-68 Complex of a Macrobicyclic Cage Amine Chelator Tethered to Two Integrin-Targeting Peptides for Diagnostic Tumor Imaging. *Bioconjugate Chem*. 2011;22(10):2093–2103. https://doi.org/10.1021/bc200319q

12. Boros E., *et al*. Acyclic chelate with ideal properties for ^{68}Ga PET imaging agent elaboration. *J. Am. Chem. Soc.* 2010;132(44):15726–15733. https://doi.org/10.1021/ja106399h

13. Sun Y., *et al*. Idum(III) and gallium(III) complexes of bis(aminoethanethiol) ligands with different denticities: stabilities, molecular modeling, and *in vivo* behavior. *J. Med. Chem.* 1996;39(2):458–470. https://doi.org/10.1021/jm9505977

14. Eder M., Krivoshein A.V., Backer M., Backer J.M. ScVEGF-PEG-HBED-CC and scVEGF-PEG-NOTA conjugates: comparison of easy-to-label recombinant proteins for [^{68}Ga]PET imaing of VEGF receptors inangiogenic vasculature. *Nucl. Med. Biol.* 2010;37(4):405–412. https://doi.org/10.1016/j.nucmedbio.2010.02.001

15. Liolios C., *et al.* Synthesis, characterization and evaluation of ^{68}Ga labelled mnomeric and dimeric quinazoline derivatives of the HBED-CC chelator targeting the epidermal growth factor receptor. *Bioorg. Chem*. 2020;100:103855. https://doi.org/10.1016/j.bioorg.2020.103855

16. Timerbaev A.R. Advances in developing tris(8-quinolinolato)gallium(III) as an anticancer drug: critical appraisal and prospects. *Metallomics.* 2009;1(3):193–198. https://doi.org/10.1039/b902861g

17. Enyedy É.A., Mészáros J.P., Spengler G., Hanif M. Comparative solution studies and cytotoxicity of gallium(III) and iron(III) complexes of 3-hydroxy-2(1H)-pyridinones. *Polyhedron.* 2019;172:141–147. https://doi.org/10.1016/j.poly.2019.04.010

18. Berry D.J., Ma Y., Ballinger J.R., Tavaré R. Efficient bifunctional gallum-68 chlators for positron emission tomography: tris(hydroxypyridinone) ligands. *ChemComm.* 2011;47(25):7068. https://doi.org/10.1039/C1CC12123E

19. Chaves S., Marques S.M., Matos A.M.F., Nunes A. New Tris(hydroxypyridinones) as Iron and Aluminium Sequestering Agents: Synthesis, Complexation and *in Vivo* Studies. *Chem. Eur. J.* 201;16(34):10535–10545. https://doi.org/10.1002/chem.201001335

20. Mathias C.J., Lewis M.R., Richert D.E., Laforest R., *et al*. Preparation of ^{66}Ga and ^{68}Ga-labeled Ga(III)-deferoxamine folate as potential folate-receptor-targeted PET radiopharmaceuticals. *Nucl. Med. Biol.* 2003;30(7):725–731. https://doi.org/10.1016/s0969-8051(03)00080-5

21. Vosjan M.J.W.D., Perk L.R., Roovers R.C., Visser G.W.M., *et al.* Facile labelling of an anti-epidermal growth factor receptor Nanobody with ^{68}Ga via a novel bifunctional desferal chelate for immuno-PET. *Eur. J. Nucl. Med. Mol. Imaging.* 2011;38(4):753–763. https://doi.org/10.1007/s00259-010-1700-1

22. Fani M., *et al*. PET of somatostatin receptor-positive tumors using ^{64}Cu- and ^{68}Ga-somatostatin antagonists: the chelate makes the difference. *J. Nuc.l Med.* 2011;52(7):1110–1118. https://doi.org/10.2967/jnumed.111.087999

23. Martell A.E., Motekaitis R.J., Clarke E.T., Delgado R., *et al*. Stability constants of metal complexes of macrocyclic ligands with pendant donor groups. *Supramol. Chem.* 1996;6(3–4):353–363. https://doi.org/10.1080/10610279608032555

24. Ma R., Welch M.J., Reibenspies J. Stability of metal ion complexes of 1,4,7-tris(2-mercaptoethyl)-1,4,7-triazacylclonane (TACN-TM) and molecular structure of In($C_{12}H_{24}N_3S_3$). *Inorg. Chim. Acta.* 1995;236(1–2):75–82. https://doi.org/10.1016/0020-1693(95)04617-I

25. Craig A.S., Parker D., Adams H. Stability, ^{71}Ga NMR, and crystal structure of a neutral gallium(III) complex of 1,4,7-triazacyclononanetriacetate: a potential radiopharmaceutical? *J. Chem. Soc., Chem. commun.* 1989;(23):1793–1794. https://doi.org/10.1039/C39890001793

26. Broan C.J., Cox J.P.L., Craig A.S., Kataky R., *et al.* Structure and solution stability of indium and gallium complexes of 1,4,7-triazacyclononanetriacetate and of yttrium complexes of 1,4,7,10-tetraazacyclododecane-tetraacetate and related ligands: kinetically stable complexes for use in imaging and radioimmunotherapy. X-Ray molecular structure of the indium and gallium complexes of 1,4,7-triazacyclononane-1,4,7-triacetic acid. *J. Chem. Soc., Perkin Trans.2.* 1991;2(1):87–99. https://doi.org/10.1039/P29910000087

27. Kruper W.J., Rudolf P.R., Langhoff C.A. Unexpected selectivity in the alkylation of polyazamacrocycles. *J. Org. Chem.* 1993;58(15):3869–3876. https://doi.org/10.1021/jo00067a018

28. Chappell L.L., Rogers B.E., Khazaeli M.B., Mayo M.S. Improved synthesis of the bifunctional chelating agent 1,4,7,10-tetraaza-*N*-(1-carboxy-3-(4-nitrophenyl)-propyl)-*N′*,*N″*,*N‴*-*tris*(acetic acid)cyclododecane (PA-DOTA). *Bioorg. Med. Chem.* 1999;7(11):2313–2320. https://doi.org/10.1016/s0968-0896(99)00171-6

29. Prata M.I.M., Santos A.C., Geraldes C.F.G.C. Characterisation of $^{67}Ga^{3+}$ complexes of triaza macrocyclic ligands: biodistribution and clearance studies. *Nucl. Med. Biol.* 1999;26(6):707–710. https://doi.org/10.1016/s0969-8051(99)00041-4

30. Heppeler A., Froidevaux S., Mäcke H.R., Jermann E., *et al.* Radiometal-Labelled Macrocyclic Chelator-Derivatised Somatostatin Analogue with Superb Tumour-Targeting Propeties and Potential for Receptor-Mediated Internal Radiotherapy. *Chem. Eur. J.* 1999;5(7):1974–1981. https://doi.org/10.1002/(SICI)1521-3765(19990702)5:7%3C1974::AID-CHEM1974%3E3.0.CO;2-X

31. Viola N.A., Rarig R.S., Ouellette W., Doyle R.P. Synthesis, structure and thermal analysis of the gallium complex of 1,4,7,10-tetraazacyclo-dodecane-*N*,*N′*,*N″*,*N‴*-tetraacetic acid (DOTA). *Polyhedron.* 2006;25(18):3457–3462. https://doi.org/10.1016/j.poly.2006.06.039

32. Velikyan I., Beyer G.J., Långström B. Microwave-Supported Preparation of ^{68}Ga Bioconjugates with High Specific Radioactivity. *Bioconjugate Chem.* 2004;15(3):554–560. https://doi.org/10.1021/bc030078f

33. Decristoforo C., Hernandez Gonzalez I., Carlsen J., Rupprich M., *et al.* ^{68}Ga- and ^{111}In-labelled DOTA-RGD peptides for imaging of αvβ3 integrin expression. *Eur. J. Nucl. Med. Mol. Imaging.* 2008;35(8):1507–1515. https://doi.org/10.1007/s00259-008-0757-6

34. Griffiths G.L., *et al.* Reagents and methods for PET using bispecific antibody pretargeting and ^{68}Ga-radiolabeled bivalent haten-peptide-chelate conjugates. *J. Nucl. Med.* 2004;45(1):30–39.

35. Sneddon D., Cornelissen B. Emerging chelators for nuclear imaging. *Curr. Opin. Chem. Biol*. 2021;63:152–162. https://doi.org/10.1016/j.cbpa.2021.03.001

36. Al-Nahhas A., *et al.* Gallium-68 PET: a new frontier in receptor cancer imaging. *Anticancer Res.* 2007;27(6B):4087–4094.

37. AL-Nahhas A., Win Z., Szyszko T., Singh A. What can gallium-68 PET add to receptor and molecular imaging? *Eur. J. Nucl. Med. Mol. Imaging*. 2007;34(12):1897–1901. https://doi.org/10.1007/s00259-007-0568-1

38. Velikyan I., Maecke H., Langstrom B. Convenient preparation of ^{68}Ga-based PET-radiopharmaceuticals at room temperature. *Bioconjugate Chem.* 2008;19(2):569–573. https://doi.org/10.1021/bc700341x

39. André J. P., Maecke H. R., Zehnder M., Macko L. 1,4,7-Triazacyclononane-1-succinic acid-4,7-diacetic acid (NODASA): a new bifunctional chelator for radio gallium-labelling of biomolecules. *Chem. Commun.* 1998;(12):1301–1302. https://doi.org/10.1039/A801294F

40. André J.P., Mäcke H., Kaspar A., Künnecke B. *In vivo* and *in vitro* 27Al NMR studies of aluminum(III) chelates of triazacyclononane polycarboxylate ligands. *J. Inorg. Biochem.* 2002;88(1):1–6. https://doi.org/10.1016/s0162-0134(01)00340-3

41. Eisenwiener K.-P., *et al.* NODAGATOC, a new chelator-coupled somatostatin analogue labeled with [$^{67/68}$Ga] and [^{III}In] for SPECT, PET, and targeted therapeutic applications of somatostatin receptor (hsst2) expressing tumors. *Bioconjugate Chem.* 2002;13(3):530–541. https://doi.org/10.1021/bc010074f

42. Jeong J.M., *et al.* Preparation of a promising angiogenesis PET imaging agent: ^{68}Ga-labeled c(RGDyK)-isothiocyanatobenzyl-1,4,7-triazacyclononane-1,4,7-triacetic acid and feasibility studies in mice. *J. Nucl. Med.* 2008;49(5):830–836. https://doi.org/10.2967/jnumed.107.047423

43. Waldron B.P., Parker D., Burchardt C., Yufit D.S. Structure and stability of hexadentate complexes of ligands based on AAZTA for efficient PET labelling with gallium-68. *Chem. Commun.* 2017;49(6):579–581. https://doi.org/10.1039/C2CC37544C

44. Parker D., Waldron B.P. Conformational analysis and synthetic approaches to polydentate perhydro-diazepine ligands for the complexation of gallium(III). *Org. Biomol. Chem.* 2013;11(17):2827. https://doi.org/10.1039/C3OB40287H

45. Costa J., Delgado R. Metal complexes of macrocyclic ligands containing pyridine. *Inorg. Chem.* 1993;32(23):5257–5265. https://doi.org/10.1021/ic00075a052

46. Ferreira C.L., Lamsa E., Woods M., Duan Y. Evaluation of Bifunctional Chelates for the Development of Gallium-Based Radiopharmaceuticals. *Bioconjugate Chem.* 2010;21(3):531–536. https://doi.org/10.1021/bc900443a

47. Liu S., Edwards D.S. Bifunctional chelators for therapeutic lanthanide radiopharmaceuticals. *Bioconjugate Chem.* 2001;12(1):7–34. https://doi.org/10.1021/bc000070v

48. Moreau J., Guillon E., Pierrard J.-C., Rimbault J. Complexing Mechanism of the Lanthanide Cations Eu^{3+}, Gd^{3+}, and Tb^{3+} with 1,4,7,10-Tetrakis(carboxymethyl)-1,4,7,10-tetraazacyclododecane (dota)—Characterization of Three Successive Complexing Phases: Study of the Thermodynamic and Structural Properties of the Complexes by Potentiometry, Luminescence Spectroscopy, and EXAFS. *Chem. Eur. J.* 2004;10(20):5218–5232. https://doi.org/10.1002/chem.200400006

49. Eder M., *et al.* Tetrafluorophenolate of HBED-CC: a versatile conjugation agent for ^{68}Ga-labeled small recombinant antibodies. *Eur. J. Nucl. Med. Mol. Imaging.* 2008;35(10):1878–1886. https://doi.org/10.1007/s00259-008-0816-z

50. Collery P., Lechenault F., Cazabat A. Juvin E., *et al*. Inhibitory effects of gallium chloride and tris (8-quinolinolato) gallium(III) on A549 human malignant cell line. *Anticancer Res.* 2000;20(2A):955–8.

51. Lessa J.A., Parrilha G.L., Beraldo H. Gallium complexes as new promising metallodrug candidates. *Inorg. Chim. Acta.* 2012;393:53–63. https://doi.org/10.1016/j.ica.2012.06.003

52. Litecká M., Hreusová M., Kašpárková J., Gyepes R., *et al.* Low-dimensional compounds containing bioactive ligands. Part XIV: High selective antiproliferative activity of tris(5-chloro--8-quinolinolato)-gallium(III) complex against human cancer cell lines. *Bioorg. Med. Chem Lett*. 2020;30(13):127206. https://doi.org/10.1016/j.bmcl.2020.127206

53. Gómez-Ruiz S., Ceballos-Torres J., Prashar S., Fajardo M. One ligand different metal complexes: Biological studies of titanium(IV), tin(IV) and gallium(III) derivatives with the 2,6-dimethoxypyridine-3-carboxylato-ligand. *J. Organometallic Chem.* 2011;696(20):3206–3213. https://doi.org/10.1016/j.jorganchem.2011.06.036

54. Chaves S., Marques S.M., Matos A.M.F., Nunes A., *et al.* New Tris(hydroxypyridinones) as Iron and Aluminium Sequestering Agents: Synthesis, Complexation and *in Vivo* Studies. *Chem. Eur. J.* 2010;16(34):10535–10545. https://doi.org/10.1002/chem.201001335

55. Chaves S., Mendonça A.C., Marques S.M., Prata M.I. A gallium complex with a new tripodal tris-hydroxypyridinone for potential nuclear diagnostic imaging: solution and *in vivo* studies of ^{67}Ga-labeled species. *J. Inorg. Biochem.* 2011;105(1):31–38. https://doi.org/10.1016/j.jinorgbio.2010.09.012

56. Smith-Jones P.M., Stolz B., Bruns C., *et al.* Gallium-67/gallium-68-[DFO]-octreotide—a potential radiopharmaceutical for PET imaging of somatostatin receptor positive tumors: synthsis and radiolabeling *in vitro* and preliminary *in vivo* studies. *J. Nucl. Med.* 1994;35(2):317–325.

57. Mathias C.J., *et al*. Receptor-mediated targeting of ^{67}Ga-deferoxamine-folate to folate-receptor-positive human KB tumor xenografts. *Nucl. Med. Biol.* 1999;26(1):23–25. https://doi.org/10.1016/S0969-8051(98)00076-6

58. Price T.W., *et al*. Evaluation of a bispidine-based chelator for gallium-68 and of the porphyrin conjugate as PET/PDT theranostic agent. *Chem. Eur. J.* 2020;26(34):7602–7608. https://doi.org/10.1002/chem.201905776

59. Imberti C., *et al.* Manipulating the *in Vivo* Behaviour of ^{68}Ga with Tris(Hydroxypyridinone) Chelators: Pretargeting and Blood Clearance. *Int. J. Mol. Sci.* 2020;21(4):1496. https://doi.org/10.3390/ijms21041496

60. Zhou X., *et al*. Design and synthesis of a new conjugate of a tris(3-hydroxy-4-pyridinone) chelator (KC18) for potential use as gallium-68-labeled prostate-specific membrane antigen (PSMA) radiopharmaceutical. *Results in Chemistry.* 2021;3:100240. https://doi.org/10.1016/j.rechem.2021.100240

61. Kowol C.R., Berger R., Eichinger R., Roller A., *et al.* Gallium(III) and Iron(III) Complexes of α-*N*-Heterocyclic Thiosemicarbazones: Synthesis, Characterization, Cytotoxicity, and Interaction with Ribonucleotide Reductase. *J. Med. Chem.* 2007;50(6):1254–1265. https://doi.org/10.1021/jm0612618

62. Arion V.B., *et al.* Synthesis, structure, spectroscopic and *in vitro* antitumour studies of a novel gallium(III) complex with 2-acetylpyridine (4)*N*-dimethylthiosemicarbazone. *J. Inorg. Biochem.* 2002;91(1):298–305. https://doi.org/10.1016/S0162-0134(02)00419-1

63. Qi J., Yao Q., Qian K., Tian L., *et al.* Gallium(III) complexes of α-*N*-heterocyclic piperidyl-thiosemicarbazones: Synthesis, structure-activity relationship, cellular uptake and activation of caspases-3/7/9. *J. Inorg. Biochem.* 2018;186:42–50. https://doi.org/10.1016/j.jinorgbio.2018.05.005

64. Qi J., *et al.* Synthesis, antiproliferative activity and mechanism of gallium(III)-thiosemicarbazone complexes as potential anti-breast cancer agents. *Eur. J. Med. Chem.* 2018;154:91–100. https://doi.org/10.1016/j.ejmech.2018.05.016

65. Firmino G. dos S.S., André S.C., Hastenreiter Z., Campos V.K., *et al. In vitro* assessment of the cytotoxicity of Gallium(III) complexes with Isoniazid-Derived Hydrazones: Effects on clonogenic survival of HCT-116 cells. *Inorganica Chim. Acta*. 2019;497:119079. https://doi.org/10.1016/j.ica.2019.119079

66. Kumar K., *et al*. Highly potent anti-proliferative effects of a gallium(III) complex with 7-chloroquinoline thiosemicarbazone as a ligand: synthesis, cytotoxic and antimalarial evaluation. *Eur. J. Med. Chem.* 2014;86:81–86. https://doi.org/10.1016/j.ejmech.2014.08.054

67. Doot R.K., Young A.J., Daube-Witherspoon M.E., Alexoff D., Labban K.J., Lee H., Wu Z., Zha Z., Choi S.R., Ploessl K.H. Biodistribution, dosimetry, and temporal signal-to-noise ratio analyses of normal and cancer uptake of [^{68}Ga] Ga-P15-041, a gallium-68 labeled bisphosphonate, from first-in-human studies. *Nucl. Med. Biol*. 2020;86:1–8. https://doi.org/10.1016/j.nucmedbio.2020.04.002

About the authors:

Anna G. Polivanova, Cand. Sci. (Chem.), Associate Professor, Department of Chemistry and Technology of Biomedical Preparations, Mendeleev University of Chemical Technology of Russia (9, Miusskaya pl., Moscow, 125047, Russia). E-mail: zagchem@mail.ru. https://orcid.org/0000-0003-4502-0745

Inna N. Solovieva, Cand. Sci. (Chem.), Associate Professor, Department of Chemistry and Technology of Biomedical Preparations, Mendeleev University of Chemical Technology of Russia (9, Miusskaya pl., Moscow, 125047, Russia). E-mail: solandsol@yandex.ru. https://orcid.org/0000-0002-0079-6710

Dmitrii O. Botev, Master Student, Department of Chemistry and Technology of Biomedical Preparations, Mendeleev University of Chemical Technology of Russia (9, Miusskaya pl., Moscow, 125047, Russia). E-mail: botev.dm@gmail.com. https://orcid.org/0000-0003-4954-6779

Danil Yu. Yuriev, Master Student, Leading Engineer, Department of Chemistry and Technology of Biomedical Preparations, Mendeleev University of Chemical Technology of Russia (9, Miusskaya pl., Moscow, 125047, Russia). E-mail: danilyuriev35@yandex.ru. https://orcid.org/0000-0002-5906-4020

Alyona N. Mylnikova, Leading Engineer, Assistant, Department of Chemistry and Technology of Biomedical Preparations, Mendeleev University of Chemical Technology of Russia (9, Miusskaya pl., Moscow, 125047, Russia). E-mail: pobeg_is_raya@mail.ru. https://orcid.org/0000-0002-8297-8322

Maxim S. Oshchepkov, Dr. Sci. (Chem.), Head of the Department of Chemistry and Technology of Biomedical Preparations, Mendeleev University of Chemical Technology of Russia (9, Miusskaya pl., Moscow, 125047, Russia). E-mail: maxim.os@mail.ru. Scopus Author ID 50262866400, ResearcherID AAA-6443-2022, https://orcid.org/0000-0002-2892-4884

Об авторах:

Поливанова Анна Геннадьевна, к.х.н., доцент кафедры химии и технологии биомедицинских препаратов Российского химико-технологического университета им. Д.И. Менделеева (125047, Россия, Москва, Миусская площадь, д. 9). E-mail: zagchem@mail.ru. https://orcid.org/0000-0003-4502-0745

Соловьёва Инна Николаевна, к.х.н., доцент кафедры химии и технологии биомедицинских препаратов Российского химико-технологического университета им. Д.И. Менделеева (125047, Россия, Москва, Миусская площадь, д. 9). E-mail: solandsol@yandex.ru. https://orcid.org/0000-0002-0079-6710

Ботев Дмитрий Олегович, магистрант, кафедра химии и технологии биомедицинских препаратов Российского химико-технологического университета им. Д.И. Менделеева (125047, Россия, Москва, Миусская площадь, д. 9). E-mail: botev.dm@gmail.com. https://orcid.org/0000-0003-4954-6779

Юрьев Данил Юрьевич, магистрант, ведущий инженер, кафедра химии и технологии биомедицинских препаратов Российского химико-технологического университета им. Д.И. Менделеева (125047, Россия, Москва, Миусская площадь, д. 9). E-mail: danilyuriev35@yandex.ru. https://orcid.org/0000-0002-5906-4020

Мыльникова Алёна Николаевна, ведущий инженер, ассистент, кафедра химии и технологии биомедицинских препаратов Российского химико-технологического университета им. Д.И. Менделеева (125047, Россия, Москва, Миусская площадь, д. 9). E-mail: pobeg_is_raya@mail.ru. https://orcid.org/0000-0002-8297-8322

Ощепков Максим Сергеевич, д.х.н., заведующий кафедрой химии и технологии биомедицинских препаратов Российского химико-технологического университета им. Д.И. Менделеева (125047, Россия, Москва, Миусская площадь, д. 9). E-mail: maxim.os@mail.ru. Scopus Author ID 50262866400, ResearcherID AAA-6443-2022, https://orcid.org/0000-0002-2892-4884

The article was submitted: March 22, 2022; approved after reviewing: April 18, 2022; accepted for publication: April 22, 2022.

The text was submitted by the authors in English.
Edited for English language and spelling by Thomas Beavitt.